SYN-EXHUMATION COUPLING OF OCEANIC AND CONTINENTAL UNITS ALONG THE WESTERN EDGE OF THE ALPINE CORSICA: A REVIEW

Maria Di Rosa*, Chiara Frassi*, Alessandro Malasoma**, Michele Marroni*,°,✉, Francesca Meneghini*
and **Luca Pandolfi*,°**

  * *Dipartimento di Scienze della Terra, Università di Pisa, Italy.*
** *Ts Lab & Geoservices Snc., Pisa, Italy.*
  ° *Istituto di Geoscienze e Georisorse, IGG-CNR, Pisa, Italy.*
  ✉ *Corresponding author, e-mail: michele.marroni@unipi.it*

ABSTRACT

The Alpine Corsica represents a segment of the Alpine collisional belt. In its western edge, it is characterized by the close association of continental units deformed under high-pressure metamorphic conditions (Lower Units) and oceanic units showing a metamorphism ranging from high-pressure (Schistes Lustrés Complex) to very low-grade conditions (Upper Units). This paper provides a complete review of the relationships between the continental and oceanic units in selected five areas where the stratigraphic features, deformation history, metamorphic P-T path and tectonic setting are available for each unit. The collected data indicate that the oceanic units occur not only at the top of the continental ones, as generally proposed in the literature, but also intercalated within them. Such relationships were achieved at shallow structural level during the late stage of exhumation, when the continental units were tectonically coupled with the oceanic units which were dragged as slices from the orogenic wedge. The coupling probably occurred immediately before the transition from syn- to post-orogenic geodynamic regime that affected the whole Alpine-Apennine collisional system in the early Oligocene. After the coupling, the stack of oceanic and continental units experienced a further exhumation-related deformation before their final exposure at the surface.

INTRODUCTION

The Alpine belt preserved in Corsica (Fig. 1) includes a stack of oceanic and continental units generated by subduction, accretion and collision between the Europe and Adria margins active from Late Cretaceous up to Oligocene (Boccaletti et al., 1971; Elter and Pertusati, 1973; Treves, 1984; Doglioni et al., 1998; Malavieille et al., 1998; Malusà et al., 2009; Marroni et al., 2010; 2017; Molli and Malavieille, 2011). The collision was preceded by a phase of continental subduction that resulted in the deformation and high-pressure metamorphism of several continental units. During the collision these continental units were closely juxtaposed with the oceanic units previously accreted during the oceanic subduction.

Several contributions have been devoted to the structural setting of the Alpine Corsica since the past century (Gibbons and Horak, 1984; Lahondère and Guerrot, 1997; Malavieille et al., 1998; Tribuzio and Giacomini, 2002; Molli, 2008; Vitale Brovarone and Herwartz, 2013; Rossetti et al., 2015; Di Rosa et al., 2017b), but the relationships between oceanic and continental units have received only little attention. Thrusting of the oceanic units onto the continental ones was interpreted as the result of a single east-dipping, ductile to brittle shear zone (Durand-Delga, 1984; Gibbons and Horak, 1984; Bezert and Caby, 1988; Jolivet et al., 1990; 1998; Molli, 2008; Maggi et al., 2012). Only recently, the relationships between oceanic and continental units along the western edge of Alpine Corsica have been described in detail from map- to the micro-scale (Molli et al., 2006; 2017; Rossetti et al., 2015; Di Rosa et al., 2017a; 2017b; 2020), revealing complex mutual relationships, with multiple slicing of oceanic and continental units.

The aim of this paper is to review the structural and metamorphic relationships between the oceanic and continental units along the whole western edge of the Alpine Corsica from south to north, i.e. from Ghisoni to North Balagne area. We will first revise stratigraphic, structural and metamorphic features of the units and then resume the tectonic setting of five key-areas along the Alpine Corsica's western edge that was previously studied by several authors (Marroni and Pandolfi, 2003; Malasoma et al., 2006; Malasoma and Marroni, 2007, Pandolfi et al., 2016; Di Rosa et al., 2017a; 2017b; 2019a; 2019b; 2019c; 2020; Malasoma et al., 2020), with the aim to provide a clear picture of the complex relationships between oceanic and continental units. Finally, all these data are placed in a tectonic model to explain the observed relationships in the framework of the Alpine Corsica geodynamic evolution.

GEODYNAMIC BACKGROUND

Corsica Island is traditionally described as geologically divided into two domains, i.e. Hercynian and Alpine Corsica, exposed in the south-west and north-east side of the island, respectively (Fig. 2). Specifically, the Alpine tectonic stack overthrusts the Hercynian domain (e.g., Durand-Delga, 1984) through a NNW-SSE trending, high-angle thrust that runs across the entire island (Fig. 2).

The Hercynian Corsica (Figs. 2 and 3), considered as representative of the European continental margin, consists of a polymetamorphic basement recording Panafrican and Variscan events intruded by Permo-Carboniferous magmatic rocks (Cabanis et al., 1990; Ménot and Orsini, 1990; Laporte et al., 1991; Rossi et al., 1994; Paquette et al., 2003; Rossi et al., 2009). The basement is covered by sedimentary successions of Mesozoic sedimentary rocks (mainly carbonates) unconformably covered by siliciclastic turbidites of Tertiary
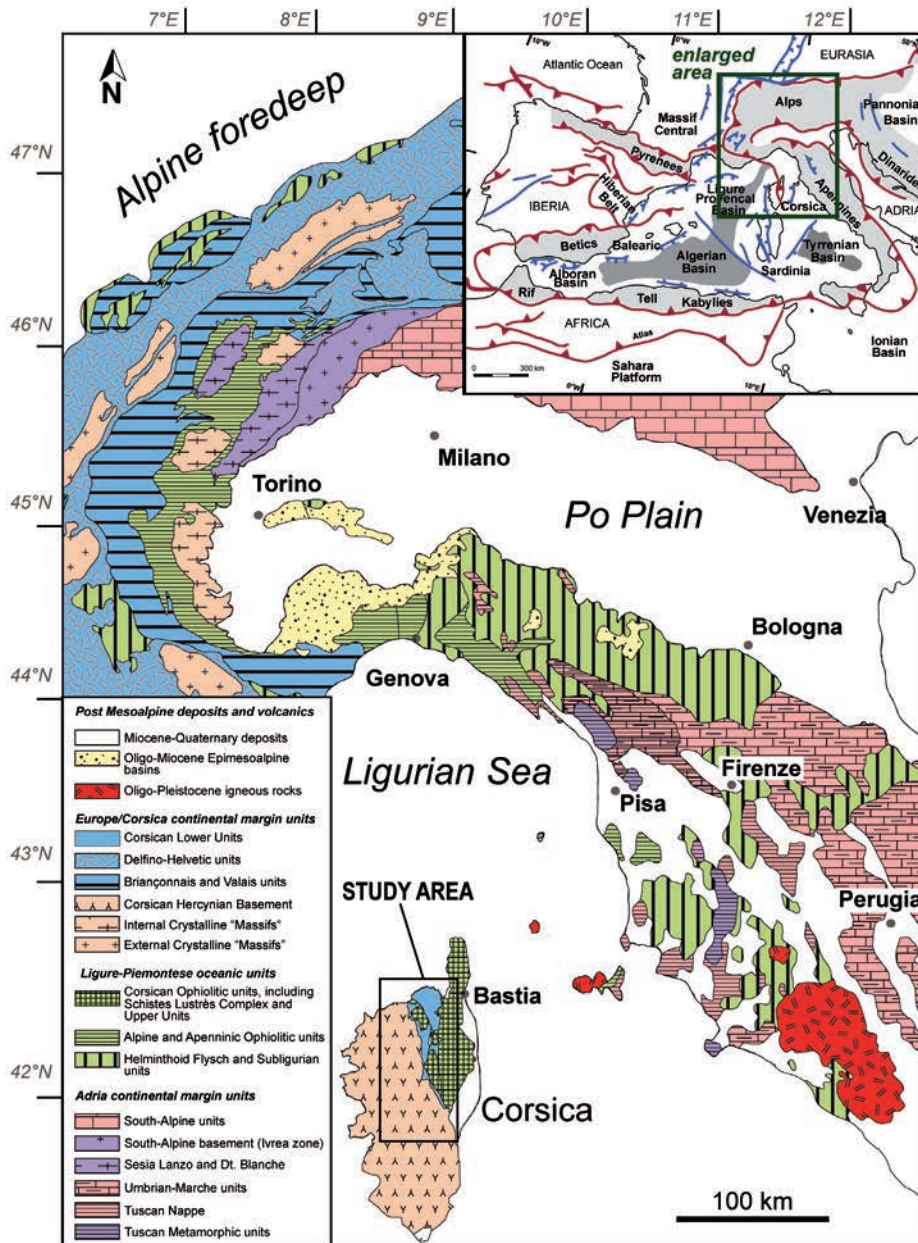
Fig. 1 - Tectonic sketch map of the Alps-Apennines-Corsica. The boxed area indicates the study area (modified from Marroni et al., 2015).

age (Durand-Delga, 1984; Rossi et al., 1994; Ferrandini et al., 2010; Di Rosa et al., 2019b; 2019c).

The Alpine Corsica (Figs. 2 and 3) comprises continental, transitional and oceanic units strongly deformed and affected by a metamorphism ranging from sub-greenschist to blue-schist-eclogite facies (e.g., Boccaletti et al., 1971; Durand-Delga, 1974; 1984; Mattauer and Proust, 1975; 1976; Amaudric du Chaffaut and Saliot, 1979; Mattauer et al., 1981; Dallan and Nardi, 1984; Gibbons and Horak, 1984; Bezert and Caby, 1988; Malavieille et al., 1998; Marroni and Pandolfi, 2003; Malasoma et al., 2006; Levi et al., 2007; Vitale Brovarone et al., 2012).

The present-day architecture of the Corsica Island has been mainly shaped by the Alpine geodynamic history started in the Middle Jurassic with the opening of the Ligure-Piemontese oceanic basin (i.e. the Western Tethys) between European and Adria continental margins (Favre and Stampfli, 1992; Manatschal, 1995; Froitzheim and Manatschal, 1996; Bill et al., 1997; Marroni and Pandolfi, 2007). The opening of

the Ligure-Piemontese oceanic basin was preceded by continental rifting of Early to Middle Jurassic age. The late stage extensional activity was dominated by a detachment fault system involving continental domain previously affected by polyphase deformation during the Variscan orogeny (Lavier and Manatschal, 2006; Marroni and Pandolfi, 2007; Péron-Pinvidic and Manatschal, 2009; Mohn et al., 2012; Beltrando et al., 2013; Masini et al., 2013; Ribes et al., 2019). The spreading phase started in Middle Jurassic, probably during the Bajocian, and developed, up to the uppermost Late Jurassic, as a magma-poor, slow-spreading mid-ocean ridge system, producing an oceanic basin not wider than 400-500 km (Abbate et al., 1980; Treves and Harper, 1994; Lagabrielle and Lemoine, 1997; Principi et al., 2004; Marroni and Pandolfi, 2007; Donatio et al., 2013; Sanfilippo and Tribuzio, 2013). From Early to Late Cretaceous, the Ligure-Piemontese oceanic basin experienced a long-lived stage of quiet without evidence of contractional or extensional tectonics. In the uppermost Late Cretaceous, during Campanian-Maastrichtian,
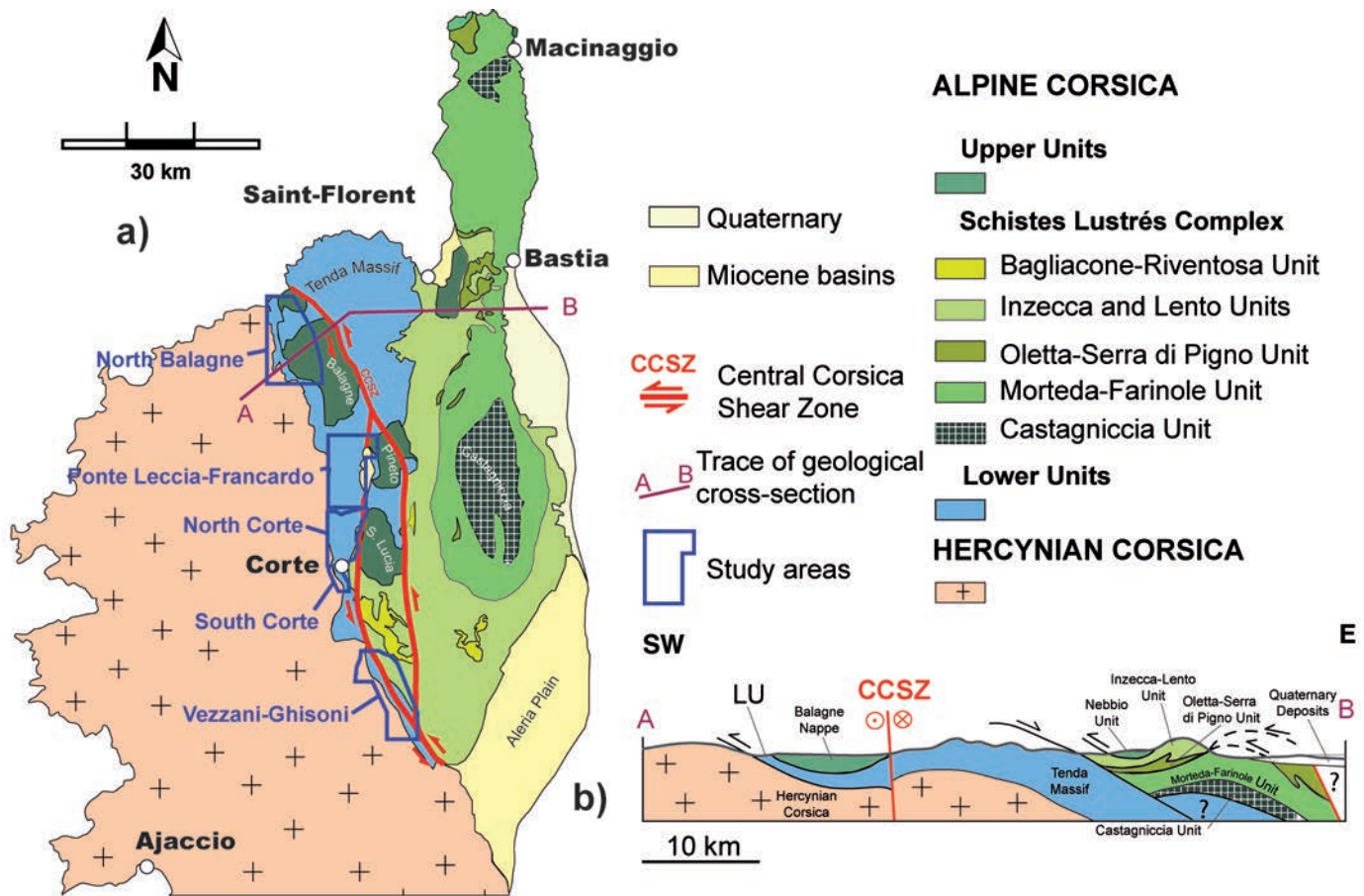
Fig. 2 - a) Tectonic sketch map of the northern Corsica (modified after Di Rosa et al., 2020) showing the location of the five areas studied in this work. b) schematic cross section.

the NW-SE directed convergence between Europe and Adria plates produced the SE-directed subduction of the Ligure-Piemontese oceanic lithosphere below the Adria continental margin (Elter and Pertusati, 1973; Lagabrielle and Polino, 1988; Schmid et al, 1996; Michard et al., 2002; Molli, 2008; Handy et al., 2010; Malusà et al., 2015; Marroni et al., 2017). Although this model is accepted by most authors, an alternative interpretation suggests that the closure of the Ligure-Piemontese oceanic basin occurred by NW-dipping subduction beneath Europe plate since the Late Cretaceous (Principi and Treves, 1984; Lahondère and Guerrot, 1997; Jolivet et al., 1998; Brunet et al., 2000). According to the former model, the thinned continental margin of the Europe plate was initially involved in the subduction zone, followed by collision with the Adria margin between Middle-Late Eocene (Gibbons and Horak, 1984; Bezert and Caby, 1988; Malavieille et al., 1998; Malasoma et al., 2006; Molli et al., 2006; Malasoma and Marroni, 2007; Maggi et al., 2012; Di Rosa et al., 2017b; 2019b). Shortly thereafter, the geodynamic scenario radically changed as a result of the post-30 Ma change of the convergence direction of the Adria-Africa plate from NW-SE to WNW-ESE (Schmid and Kissling, 2000; Ceriani et al., 2001; Handy et al., 2010; Malusà et al., 2015). This change induced the underthrusting of the southern part of the Ligure-Piemontese oceanic basin beneath the European continental margin starting from early Oligocene (Rosenbaum et al., 2002; Faccenna et al., 2004). The onset of the Apennine orogeny is typically marked by this subduction polarity inversion, that led to the progressive deformation of the

Adria continental margin, i.e. the Apennine slab (Réhault et al., 1984; Doglioni, 1991; Gueguen et al., 1998). As a consequence, Corsica underwent two major extensional stages, both related to the rollback of the Apennine slab (Gueguen et al., 1998; Chamot-Rooke et al., 1999; Faccenna et al., 2004; Fellin et al., 2005). The first stage was related to the early Oligocene opening of the Liguro-Provençal oceanic basin which separated the Corsica-Sardinia continental microplate from the neighbouring domains of the Alpine collisional belt. The spreading of the Liguro-Provençal oceanic basin, that spanned from Aquitanian to Langhian, was coupled to a counterclockwise rotation of around 55° of the Corsica-Sardinia continental microplate (Gattacceca et al., 2007). The second stage was linked to the late Miocene opening of the Tyrrhenian Sea which, in turn, isolated the Corsica-Sardinia continental microplate from the Adria plate. As result of these events, the contractional tectonics in Corsica was followed in the early Oligocene by large-scale extension, leading the collapse of the previously thickened orogenic wedge (Jolivet et al., 1991; Fournier et al., 1991; Jolivet et al., 1991; 1998; Daniel et al., 1996; Brunet et al., 2000; Jakni et al., 2000; Zarki-Jakni et al., 2004; Pandeli et al., 2018).

Since the intuition of Argand (1924) and Staub (1924), the Alpine Corsica has been regarded as linked to the Western Alps belt which shared the same evolution until early Oligocene (e.g., Mattauer et al., 1981; Durand-Delga, 1984; Marroni and Pandolfi, 2003; Faccenna et al., 2004; Molli and Tribuzio, 2004; Molli et al., 2006; Handy et al., 2010; Molli and Malavieille, 2011; Gueydan et al., 2017).

74

The subduction and collision evolution is fully identifiable in the tectono-metamorphic history recorded in the Alpine Corsica (e.g., Mattauer et al., 1981; Durand-Delga 1984) Similarly to Western Alps, the development of an accretionary wedge composed of oceanic and transitional (oceanic-continental) units with high-pressure (HP) metamorphic imprint starting from Late Cretaceous, is well testified also in the Alpine Corsica (e.g., Mattauer et al., 1977; Caron and Delcey, 1979; Caron et al., 1981; Faure and Malavieille, 1981; Lahondère et al., 1983; Harris, 1985; Warburton, 1986; Waters, 1990; Fournier et al., 1991; Jolivet et al., 1991; Caron, 1994; Guieu et al., 1994; Lahondère and Guerrot, 1997; Malavieille et al., 1998; Tribuzio and Giacomini, 2002; Levi et al., 2007; Chopin et al., 2008; Ravna et al., 2010; Vitale Brovarone et al., 2012; 2014; Meresse et al., 2012). Likewise, the oceanic units characterized by very low-grade metamorphism are considered as involved in the convergence-related deformations at higher structural level (Durand-Delga et al., 1997; Saccani et al., 2000; Marroni and Pandolfi, 2003; Pandolfi et al., 2016).

Involvement of the European continental margin in the subduction led to the detachment of continental crust fragments from the downgoing plate and their accretion to the wedge as deformed and metamorphosed slices (e.g., Gibbons and Horak, 1984; Bezert and Caby, 1988; Egal, 1992; Chemenda et al., 1995; Daniel et al., 1996; Brunet et al., 2000; Tribuzio and Giacomini, 2002; Gueydan et al., 2003; Malasoma et al., 2006; Molli et al., 2006; Malasoma and Marroni, 2007; Garfagnoli et al., 2009; Molli and Malavieille, 2011; Maggi et al., 2012; Di Rosa et al., 2017b; 2019b; 2019b).

TECTONIC SETTING OF ALPINE CORSICA

The Alpine Corsica (Fig. 2a) is formed by a stack of tectonic units, that are classically divided in three groups according to their stratigraphic, structural and metamorphic
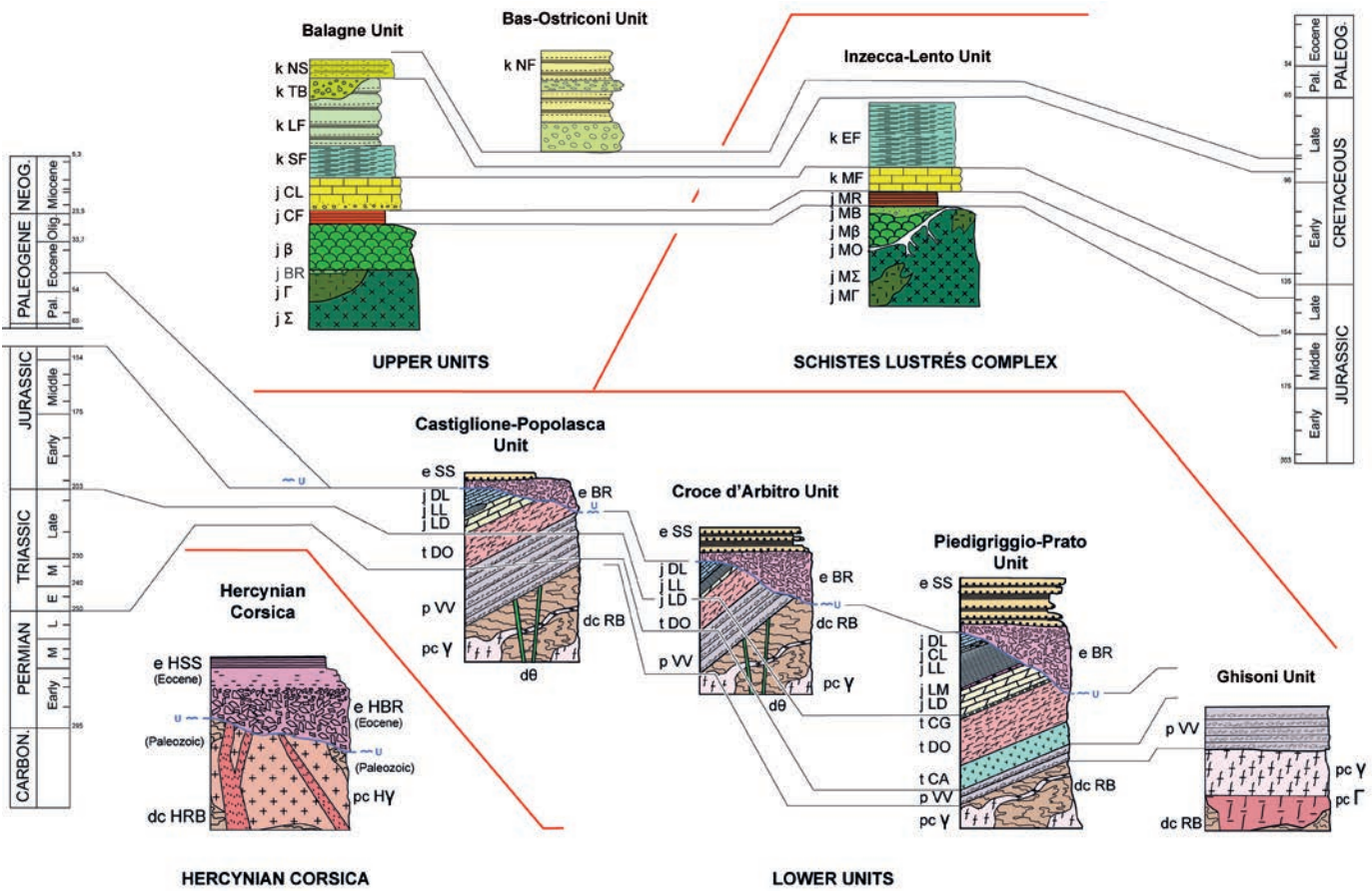

Fig. 3 - Reconstructed stratigraphic logs of the studied units.
Key: (HERCYNIAN CORSICA), dcHRB- Roches Brunes Fm. (Devonian-Carboniferous), pHcγ -Metagranitoids (Permo-Carboniferous); eHBR- Breccia Fm. (middle to late Eocene); eSS- Sandstone Fm. (middle to late Eocene). (LOWER UNITS), dcRB- Roches Brunes Fm. (Devonian-Carboniferous); pcγ- Metagranitoids (Permo-Carboniferous); pcΓ- Metagabbros (Permo-Carboniferous); pVV-Metavolcanic and Metavolcaniclastic Fm. (Permian); tCA- Meta-carniole Fm. (Carnian); tDO- Lower Metadolostone Fm. (Norian); tCG- Metaconglomerate Fm. (Rhaetian); jLD-Metalimestone and Metadolostone Fm. (Hettangian-Sinemurian); jLM- Lumachella Metalimestone Fm. (Hettangian-Sinemurian); jLL- Laminated Metalimestone Fm. (Lias); jCL-Cherty Metalimestone Fm. (Lias); jDL- Detritic Metalimestone Fm. (Lias); eBR- Metabreccia Fm. (middle to late Eocene); eSS- Metasandstone Fm. (middle to late Eocene). (SCHISTES LUSTRÉS COMPLEX), jMΣ-Metaserpentinites and metaperidotites (Middle to Late Jurassic); jMΓ- Metagabbros (Middle to Late Jurassic); jMO- Metaophicalcites (Middle to Late Jurassic); jMβ- Metabasalts (Middle to Late Jurassic); jMB- Metaophiolite breccias (Middle to Late Jurassic); jMR-Metaradiolarite Fm. (Late Jurassic); kMF- Marble Fm. (Early Cretaceous); kEF- Erbajolo Fm. (Middle-Late Cretaceous). (UPPER UNITS), jΣ - serpentinized lherzolites (Middle-Late Jurassic); jΓ gabbros (Middle-Late Jurassic); jBR- ophiolite-bearing breccia (Middle-Late Jurassic); jβ pillow basalt (Middle-Late Jurassic); jCF- Chert (middle Callovian-Kimmeridgian); jCL- Calpionella Limestone (Tithonian-early Berriasian); kSF- San Martino Fm. (early Berriasian-late Hauterivian/early Barremian); kLF- Lydienne Flysch (late Hauterivian/early Barremian-early Turonian); kTB-Toccone Breccia (late Cenomanian); kNS-Novella Sandstone (late Cenomanian); kNF-Narbinco Flysch (not older than latest Coniacian, ? Campanian).

features (e.g., Durand-Delga, 1984; Jolivet et al., 1990; Malavieille et al., 1998; Marroni and Pandolfi, 2003; Molli, 2008). From bottom to the top, the Lower Units (also known as "Prépiemontais Units"), the Schistes Lustrés Complex and the Upper Units (also known as "Nappe Supérieure") have been recognized. Each group of units represents a specific paleogeographic and/or paleotectonic domain in the context of the Alpine evolution.

The Lower Units (Figs. 2 and 3), hereafter referred as LU (i.e. Tenda Massif, Volparone Breccia Slice and Palasca-Moltifao, Fuata-Pedanu, Castiglione-Popolasca, Croce d'Arbitro, Piedigriggio-Prato, Canavaggia, Pedani, Scoltola, Ghisoni Units), are continental-derived units unambiguously considered as fragments of the thinned European continental margin (i.e. comparable with the current Corsica-Sardinia continental microplate) accreted at various depths to the Alpine orogenic wedge in Tertiary time (Amaudric du Chaffaut, 1975; Amaudric du Chaffaut et al., 1976; Amaudric du Chaffaut and Saliot, 1979; Bezert and Caby, 1988; Egal and Caron, 1988; Egal, 1992; Tribuzio and Giacomini, 2002; Molli and Tribuzio, 2004; Molli et al., 2006; Malasoma et al., 2006; Malasoma and Marroni, 2007; Di Rosa et al., 2017a; 2017b; 2019b; 2019c).

The Schistes Lustrés Complex (Fig. 2a), hereafter referred to as SL, includes oceanic and continental units deriving from paleogeographic domains corresponding to the Ligure-Piemontese oceanic basin and its transition to the European continental margin (Caron and Delcey, 1979; Mattauer et al., 1981; Faure and Malavieille, 1981; Pequignot, 1984; Jolivet et al., 1990; Fournier et al.,1991; Lahondère et al., 1999). They therefore represent fragments of oceanic and ocean-continent transition lithosphere (Rosenbaum et al., 2002; Mohn et al., 2009; Agard et al., 2011; Vitale Brovarone et al., 2014; Deseta et al., 2014), deformed since the Late Cretaceous and exhumed in the Tertiary (Jolivet, 1993). Given the complex stratigraphy and the variable metamorphic imprints that characterize the SL, several classifications have been proposed (e.g., Caron and Delcey, 1979; Padoa, 1999; Rossi et al., 2001; Marroni et al., 2004; Levi et al., 2007; Vitale Brovarone et al., 2012; Vitale Brovarone and Hewartz, 2013). Specifically, along the western edge of the Alpine Corsica the SL are represented by the Inzecca Unit (Cf. Lento Unit by Rossi et al., 1994 and Levi et al., 2007), hereafter referred as Inzecca-Lento Unit.

The Upper Units (Fig. 2a), hereafter referred to as UU, consist of oceanic units (including Balagne Nappe and Nebbio, Macinaggio, Rio Magno, Bas-Ostriconi, Serra Debbione-Pineto Units) with a reconstructed stratigraphy comprising an ophiolite sequence with its sedimentary cover and carbonate turbidites, deformed under very low-grade metamorphic conditions (e.g., Mattauer et al., 1981; Dallan and Nardi, 1984; Durand-Delga, 1984; Waters, 1990; Fournier et al., 1991; Dallan and Puccinelli, 1995; Daniel et al., 1996; Malavieille et al., 1998; Marroni and Pandolfi, 2003; Molli and Malavieille, 2011; Pandolfi et al., 2016).

The current tectonic stack of LU, SL and UU appears to be locally dissected by an important fault system called "Central Corsica Shear Zone (CCSZ)" by Waters (1990) and "Ostriconi Fault" by Lacombe and Jolivet (2005). The main fault has a sinistral strike-slip kinematics and locally overprints the boundary between Alpine and Hercynian Corsica (Lacombe and Jolivet, 2005; Di Rosa et al., 2017a; 2017b). Sinistral synthethic and dextral antithethic systems are associated with the main fault, further complicating the mutual relationships between the units of the different groups. The age

of the CCSZ is poorly known; its activity is constrained from Eocene (Maluski et al., 1973) to late Eocene-early Oligocene (Marroni et al., 2017) and early Miocene (Waters, 1990).

The relations between LU, SL and UU are sealed by the Burdigalian deposits cropping out in the Saint-Florent and Francardo basins and the Aleria Plain (Alessandri et al., 1977; Dallan and Puccinelli, 1995; Ferrandini et al., 1998; Cavazza et al., 2001; Cavazza et al., 2007; Gueydan et al., 2017) (Fig. 2). These basins opened during the extensional regime that affected the Corsica Island in the post-collisional phase.

The final deformation event in the Alpine Corsica is associated with map-scale folds characterized by N-S trend axes and sub-vertical axial plains (e.g., Gueydan et al., 2017). Such structures, i.e. Cap Corse and Castagniccia antiforms and Centuri, Saint-Florent and Aleria synforms, deform the Miocene deposits of Saint-Florent, Francardo and Aleria (Faure and Malavieille, 1981; Durand-Delga, 1984) and are consequently related to the late stage of the Miocene extensional tectonics (Jolivet et al., 1990; 1991; Fournier et al., 1991; Egal, 1992; Marroni and Pandolfi, 2003).

THE UNITS FROM THE WESTERN EDGE OF ALPINE CORSICA: AN OVERVIEW

In this chapter we review the stratigraphic, structural and metamorphic features of the units from the western edge of Alpina Corsica, with emphasis on five selected areas (Fig. 2), to illustrate the complex tectonic relationships among the oceanic and continental units.

North Balagne area
The North Balagne area extends from the coastline to the north (Ostriconi Beach) to the Lagani Valley in the south (Fig. 2). This area hosts an east-dipping stack of tectonic units (Rossi et al., 2001 and references therein) comprising: the Volparone Breccia Slice from the LU and the Balagne Nappe and Bas-Ostriconi Unit from the UU.

Ponte Leccia-Francardo area
This area (Fig. 2) is bounded to the north by the Asco Valley and to the south by the Golo Valley and it empasses a north-south trending and east dipping stack of the following tectonic units (Rossi et al., 1994; Malasoma et al., 2020): Castiglione-Popolasca, Croce d'Arbitro and Piedigriggio-Prato Units from the LU, Inzecca-Lento Unit of the SL, and the Serra Debbione-Pineto Unit from the UU.

North Corte area
The North Corte area (Fig. 2) is located in the center of the Corsica Island, between Castirla, Francardo and Corte. The north-south trending and east dipping stack of tectonic units comprises: Castiglione-Popolasca, Croce d'Arbitro, Piedigriggio-Prato and the Caporalino Units from the LU, and a thin slice of Inzecca-Lento Unit of the SL, cropping out around the Buttinacce Village and hereafter referred to as IZU-Buttinacce.

South Corte area
The South Corte area is located in the center of the Corsica Island, between Corte and Casanova (Fig. 2) and includes a stack of units made of: Castiglione-Popolasca Unit for the LU, the Bagliacone-Riventosa Unit of the SL, and, between them, another tectonic slice of IZU, occurring near the Village of Botro and hereafter referred to as IZU-Botro.

Vezzani-Ghisoni area

This area (Fig. 2) extends between the Villages of Vez-zani, to the north, and Ghisoni, to the south. The LU are here represented by the Ghisoni Unit sandwiched between the Hercynian Corsica and the Inzecca-Lento Unit from the SL. The boundaries among the different units are strongly over-printed by deformation related to the CCSZ.

LITHOSTRATIGRAPHY

As introduced, the LU, SL and UU include units whose re-constructed stratigraphic succession suggests their paleogeo-graphic domain of provenance, with the LU units coming from the thinned continental margin of the Europe plate, and the SL and UU belonging to the Ligure-Piemontese oceanic basin and its transition to the continental margin (Caron and Delcey, 1979; Mattauer et al., 1981; Dallan and Nardi, 1984; Durand-Delga, 1984; Jolivet et al., 1990; Waters, 1990; Fournier et al., 1991; Malavieille et al., 1998; Lahondère et al., 1999; Marroni and Pandolfi, 2003; Molli and Malavieille, 2011; Pandolfi et al., 2016). We proposed a syntethic stratigraphic chart of the LU, SL and UU, where we used all the available data collected during field work and from literature (Fig. 3).

The Lower Units (LU)

The reconstructed stratigraphic log of the LU includes a Paleozoic basement composed of metagranitoids and their host rocks, both covered by Permian volcanics and volcani-clastic deposits gradually passing to a sedimentary sequence ranging in age from Trias to Eocene (Fig. 3). The different LU in the study areas include only a part of the complete succession.

The so-called Roches Brunes Fm. makes up the basement and consists of polydeformed and polymetamorphic micas-chists, paragneiss, quartzites and amphibolites of Panafrican age (Rossi et al., 1994). The Roches Brunes Fm. is intruded by metagranitoids of Permo-Carboniferous age (Ménot and Orsini 1990; Laporte et al., 1991; Paquette et al., 2003; Rossi et al., 2015) cut by meta-aplitic dykes and covered by the Permo-Carboniferous Metavolcanic and Metavolcaniclastic Fm. The basement is unconformably covered by a metasedi-mentary succession of Mesozoic age which includes:
– Norian Lower Metadolostone Fm. (Rossi et al., 1994) made of thick layers of metadolostones intercalated with purple metapelites interpreted as paleosoil horizons;
– Rhaetian Metaconglomerate Fm. with fragments of meta-dolostones and metavolcanics in a carbonate matrix that crops out as discontinuous lenses;
– Hettangian-Sinemurian Metalimestone and Metadolos-tone Fm. consisting of medium to thick beds of metalime-stones and metadolostones;
– Hettangian-Sinemurian Lumachella Metalimestone Fm. with well-preserved fossil associations;
– Laminated Metalimestone Fm. of Liassic age (Rossi et al., 1994) represented by thin beds of metalimestones alter-nating with very thin beds of metapelites;
– Cherty Metalimestone Fm. in discontinuous lenses;
– Detritic Metalimestone Fm. of Liassic age consisting of matrix-supported polymict metabreccias, often character-ized by well graded beds.
The Mesozoic succession is unconformably topped by:
– Metabreccia Fm. (cf. Volparone Breccia of Malasoma and Marroni, 2007) formed by subrounded to subangular clasts of orthogneisses, paragneisses, micaschists, meta-granites, quartzites and marbles enclosed in a fine-grained matrix ranging in size from metapelites to metarenites;
– Metasandstone Fm. that crops out as medium beds of metarenites and metapelites. The occurrence of *Num-mulites sp.* indicates a middle to late Eocene age for this formation (Bezert and Caby, 1988; Rossi et al., 1994; Fer-randini et al., 2010).

The Schistes Lustrés Complex (SL)

Along the western edge of the Alpine Corsica the SL are represented by the Inzecca-Lento Unit, considered as repre-sentative of the oceanic lithosphere of the Ligure-Piemontese oceanic basin. Despite the polyphase deformation and the as-sociated HP metamorphism, a reconstruction of stratigraphic succession for the Inzecca-Lento Unit is possible by integrat-ing the field data with comparison to the less metamorphic succession of the UU and the Internal Ligurian Units of the Northern Apennines, as proposed in several papers (Caron and Delcey, 1979; Durand Delga, 1984; Padoa, 1999; Levi et al., 2007). The reconstructed succession (Fig. 3) includes a metaophiolite sequence of Middle to Late Jurassic age (Li et al., 2015), and a thick metasedimentary cover.

Specifically from top to bottom the succession comprises:
– a basement composed of metaperidotites intruded by sev-eral bodies of metagabbros. The metaperidotites, gener-ally highly sheared and serpentinized, are cross-cut by rare basaltic or rodingitized gabbroic dikes. In some out-crops, the metaserpentinites are topped by thin levels of metaophicalcites. The metagabbros range in composition from Mg- to Fe-gabbros, with subordinate plagiogranites (Ohnenstetter et al., 1976);
– a volcano-sedimentary complex of several hundreds to few metres in thickness that includes massive or pillowed metabasalts with MOR geochemical affinity (Saccani et al., 2008), generally associated with oceanic metabrec-cias. Locally the volcano-sedimentary complex is lacking and the metasedimentary cover is directly lying at the top of the basement;
– a metasedimentary cover, including from bottom to top:
  i) a thin succession of metaradiolarites (Metaradiolarite Fm., Late Jurassic),
  ii) very thin and discontinuous sequences of marbles (Marble Fm., Early Cretaceous), whose protolith is likely represented by the Calpionella Limestone (Levi et al., 2007),
  iii) the Cretaceous Erbajolo Fm. (Amaudric du Chaffaut et al., 1972), represented by a thick succession of dm-thick layers of micaschists and cm-thick layers of marble alternated with massive, m-thick intervals of calcschists. Near Venaco, the Erbajolo Fm. is topped by a thin level characterized by layers of micaschists, quartzites and marbles, that is in turn covered by meta-breccias, where blocks of marbles and quarzites are set in a matrix of micaschists (Amaudric du Chaffaut et al., 1985).
As a whole, the ophiolite sequence of the Inzecca-Lento Unit shows the same features of many others ophiolitic units of the Western Tethys as, for instance, the reduced thickness of the basement, lack of the sheeted dike complex, and oc-currence of ophicalcites and ophiolitic breccias (Marroni and Pandolfi, 2007). Similarly, the sedimentary cover succession can be compared with the Middle Jurassic to early Paleocene sedimentary cover of the ophiolite sequence from the Internal

Ligurian Units of Northern Apennine (Abbate et al., 1980; Principi et al., 2004; Marroni et al., 2017). The metabreccias that discontinuously occur on top of the Erbajolo Fm. may be correlated with the Bocco Shale Fm., cropping out in the Northern Apennine (Marroni and Pandolfi, 2001; Meneghini et al., 2020).

The Upper Units (UU)

The UU crop out as dismembered slices. The original stratigraphic log can be tentatively reconstructed as follows in the Balagne Nappe and Serra Debbione-Pineto Units (Fig. 3):
– a 500 m thick oceanic basement consisting of mantle peridotites intruded by gabbro bodies. The mantle rocks (i.e. serpentinized lherzolites cut by dikes of rodingitized gabbros) occur only in the Balagne Nappe. The gabbros, well exposed in the Pineto Massif, consist of a layered intrusive sequence, that includes prevailing troctolites, dunites, subordinate Mg- and Fe-gabbros, all cross-cut by rare dolerite dykes (Saccani et al., 2000; 2008; Durand-Delga et al., 2005; Sanfilippo and Tribuzio; 2013; Sanfilippo et al., 2015; Berno et al., 2019);
– a basalt complex with T-MORB affinity, typical of oceanic crust developed during the early stages of oceanic spreading (Durand-Delga et al., 1997; Saccani et al., 2000; 2008; Padoa et al., 2001; 2002). The basalts in the Balagne Nappe reach a thickness of about 500 m and occur as pillow lavas with massive bodies at their base (Rossi et al., 1994). Between basalts and gabbros a thin level of ophiolitic breccia has been also identified;
– a sedimentary cover starting with radiolarian-bearing cherts (middle Callovian-Kimmeridgian; De Wever et al., 1987);
– Calpionella Limestone (Tithonian-early Berriasian);
– San Martino Fm. (Durand-Delga, 1984), consisting of about 100 m thick marls, carbonate-free shales and silicified calcilutites of early Berriasian to late Hauterivian/early Barremian age (Marroni et al., 2000);
– Lydienne Flysch (Cf. Balliccione Flysch, Durand-Delga et al., 2005), consisting of thin-bedded mixed turbidites of late Hauterivian/early Barremian to early Turonian age (Marino et al., 1995; Marroni et al., 2000).

In the Balagne Nappe the whole succession is characterized by the presence of terrigenous debris interbedded within the whole stratigraphic log. The Calpionella Limestone is characterized by interbedding of coarse-grained debris strata showing a mixed carbonatic-siliciclastic composition (Bracciali et al., 2007; Cavazza et al., 2018). In turn, the Lydienne Flysch, up to 300 m thick, shows vertical and lateral stratigraphic transition to the Toccone Breccia and Novella (Cf. Gare de Novella) Sandstone (late Cenomanian), both consisting of coarse-grained deposits showing a carbonatic-siliciclastic composition (Bracciali et al., 2007; Cavazza et al., 2018). According to Sagri et al. (1982) and Cavazza et al. (2018), these formations represent a portion of a complex turbidite system fed by the Europe/Corsica continental margin during the Cretaceous.

Differently from Balagne Nappe and Serra Debbione-Pineto Unit, the Bas-Ostriconi Unit includes only the Late Cretaceous Narbinco Flysch consisting of carbonate turbidites with lenses of coarse-grained polymictic conglomerates. According to Marino et al. (1995), the nannofossils found in the Narbinco Flysch suggest latest Coniacian or Campanian as maximum age. The composition of the Narbinco Flysch is thus similar to that of the Lydienne Flysch, the Toccone Breccia and the Novella Sandstone (Pandolfi et al., 2016).

According to Durand-Delga (1984), Durand-Delga et al., (2005), Marroni and Pandolfi (2003) and Pandolfi et al. (2016), the UU were originated from an area of the Ligure-Piemontese oceanic basin located close to the European continental margin.

DEFORMATION HISTORY

The LU, SL and UU followed independent deformation histories until their stacking at the base of the prism, with associated HP-LT peak metamorphism for the LU and SL, and very low-grade metamorphism for the UU (Durand- Delga, 1984; Gibbons et al., 1986; Waters, 1990; Fournier et al., 1991; Egal, 1992; Caron, 1994; Daniel et al., 1996; Malavieille et al., 1998; Marroni and Pandolfi, 2003; Molli, 2008; Molli and Malavieille, 2011; Vitale Brovarone et al., 2011; Rossetti et al., 2015; Di Rosa et al., 2017a; 2017b; 2019b; 2019c; 2020). The deformation phases and the metamorphism detected in these units before their stacking have not only different ages but also different tectonic meaning.

Whereas the LU have been involved in the continental subduction in the late Eocene-Oligocene time span, the SL and UU have been deformed since Late Cretaceous during the subduction of the oceanic lithosphere but at different structural levels, deep for the SL and shallow for the UU.

The Alpine-related deformation in the LU, SL and UU is only weakly modified by subsequent events that developed at shallow structural levels. The oldest one is related to the development of the CCSZ system, whose structures are sealed by the early Miocene deposits of the Francardo Basin (Alessandri et al., 1977). In turn, the Miocene deposits are deformed by large wavelength open folds recognized only at the map scale. In this paper, these later deformations are not presentede and discussed.

Lower Units (LU)

Despite the differences in the P-T conditions of the metamorphic peak, the LU are characterized by a comparable structural setting derived from the overprinting of three phases of ductile deformations (Fig. 4), hereafter referred as D_{1LU}, D_{2LU} and D_{3LU} phases (Bezert and Caby, 1988; Egal, 1992; Malasoma et al., 2006; Malasoma and Marroni, 2007; Garfagnoli et al., 2009; Di Rosa et al., 2017a; 2017b; Di Rosa et al., 2019b; 2020). Each deformation phase is characterized by the development of pervasive folding and foliation that can be recognized from meso- to microscale. Due to progressive nature of the deformation, the structures of the D_{1LU} phase are almost completely obliterated during the subsequent D_{2LU} phase, whose structures are the most widespread in the field producing the most important map-scale structures. Differently, the last D_{3LU} phase does not produce any relevant change of the pre-existing structural setting.

D_{1LU} - In the field, relics of the D_{1LU} phase are represented by folded quartz veins and, occasionally, by sheath folds (Fig. 5a) mainly identified only in the Laminated Metalimestone Fm. in the North Corte area. In addition, rare examples of S_{1LU} foliation overprinted by the S_{2LU} in the hinges of the F_{2LU} folds have been observed mostly in Metasandstone Fm. along the old road from Bistuglio to Soveria. In the LU, from North Balagne area, no evidence of F_{1LU} folds have been recognized. At the microscopic scale, relics of the D_{1LU} phase have been recognized in several units, within the metapelite-
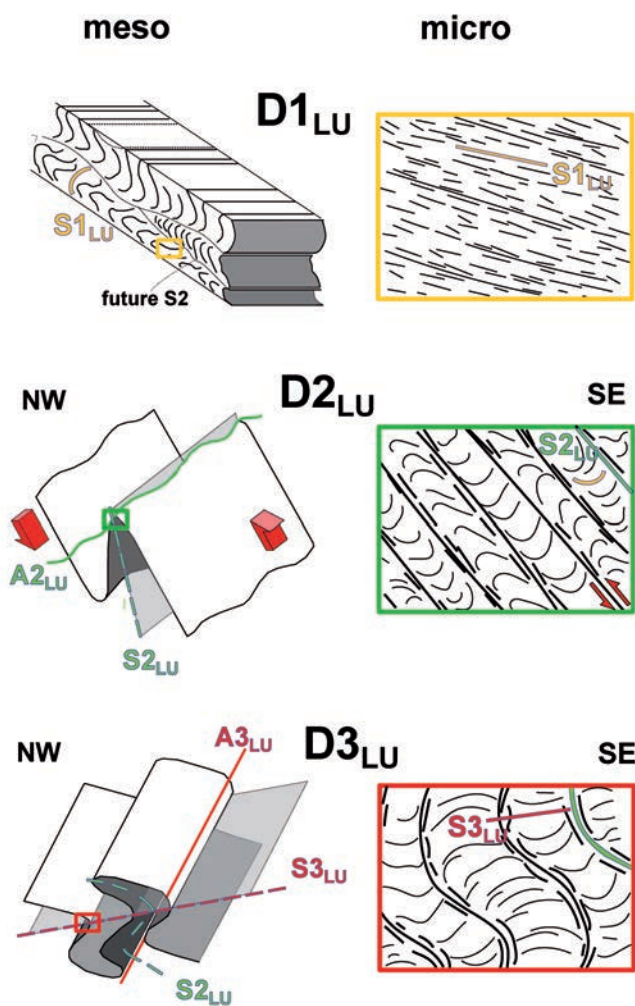
Fig. 4 - Sketches showing meso- and microscale deformation features in the Lower Units (modified after Di Rosa et al., 2019c).

bearing formations such as, for instance, the Metabreccia and the Metasandstone Fms. Here, S_{1LU} is a transposed foliation in the microlithons along the S_{2LU} foliation (Fig. 5b) defined as a schistosity locally wrapping Qz and Fsp porphyroclasts, and characterized in the metapelites by the Chl + Ph + Qz + Cal mineral assemblage (mineral abbreviations from Whitney and Evans, 2010). In the metalimestones, evidences of the D_{1LU} phase are large boudinaged calcite crystals showing twins morphology that can be ascribed to the Type 2 of Burkhard (1992) classification.

D_{2LU} - It is the most penetrative phase at the field-scale. In metalimestones, metapelites, metarenites, metabreccias and metagranitoids (Fig. 5c) the S_{2LU} foliation can be recognized as a pervasive and continuous planar anisotropy. Along the limbs of the F_{2LU} folds in the metapelites and metarenites, the S_{2LU} foliation is a schistosity, whereas in the hinge zone of F_{2LU} folds, it can be classified as a gradational to discrete spaced crenulation cleavage. In the Metabreccia Fm., the well-developed S_{2LU} foliation is highlighted by flattened coarse-grained clasts; the lithotypes occurring as clasts are metagranitoids, marbles, meta- rhyolites, micaschists and mafic rocks. The strike of the S_{2LU} foliation is quite constant in the different areas ranging from NNW-SSE in the North

Balagne area to N-S in the Ponte Leccia-Francardo, North Corte, South Corte and Vezzani-Ghisoni areas. A well-visible mineral lineation L_{2LU} on the S_{2LU} foliation is defined by elongated Chl + Qz + Ph grains, whereas in the metalimestones the L_{2LU} stretching lineations is mainly represented by boudinaged millimetric Py and elongated Qz grains with oriented growth of Cal fibres. Analogously to the strike of the foliation, the L_{2LU} lineations show a constant E-W trend in all the study areas. The S_{2LU} foliation is associated with sub-isoclinal to isoclinal F_{2LU} folds (Fig. 5d), well-developed at all scales and typically showing necking and boudinage along stretched limbs. The trend of A_{2LU} axes ranges from NNW-SSE to N-S from north to south across the study areas.

In thin sections of metapelites and metarenites sampled along the limbs of the F_{2LU} folds, principal anisotropy is a continuous and pervasive S_{2LU} - S_{1LU} composite foliation where the metamorphic minerals recrystallized during the D_{2LU} phase are superimposed on the pre-existing D_{1LU} phase minerals (Fig. 5e). In the samples from the F_{2LU} hinge-zone, the S_{2LU} foliation is a crenulation cleavage, characterized by smooth cleavage domains showing a gradational to discrete transition to the microlithons where the S_{1LU} foliation is still preserved (Fig. 5b). The S_{2LU} foliation is characterized by synkinematic recrystallization of Ph + Qz + Cal + Chl + Ab. In the metalimestones, associated to the D_{2LU} phase, pervasive calcite recrystallization occurs, with development of a fine-grained granoblastic texture.

Formation of N-S trending meter-scale shear zones is associated with D_{2LU} phase and marks the boundary between the units (Fig. 5f). Shear sense indicators such as asymmetric tails of white mica around σ- and δ-type porphyroclasts of Qz and Fsp point to a top-to-the W sense of shear. Additional kinematic indicators are S-C/C' fabrics, mica fishes, and bookshelf structures in Fsp. Locally, these units-bounding shear zones are overprinted by cataclastic deformation.

The S_{2LU} foliation in the metagranitoids from Croce d'Arbitro and Ghisoni units is a mylonitic foliation (Fig. 5g), with a mineral assemblage of Qz + K-Fsp + Pl + Chl + Ph ± Cal ± Ep ± Bt (Di Rosa et al., 2017a; 2019b), defined by discontinuous lepidoblastic layers of Ph ± Bt and granoblastic layers of fine-grained Qz + Pl. Cm-sized Qz and K-Fsp grains occur as σ-type porphyroclasts. The largest Qz grains are affected by undulatory extinction, deformation lamellae, deformation bands and bulging. Locally, Qz crystals are strongly elongated and partially recrystallized, indicating an incipient recrystallization by subgrain rotation mechanisms. These microstructures indicate that dislocational creep was the main deformation mechanism suggesting a deformation temperature < 400°C (Stipp et al., 2002).

D_{3LU} - This phase presented open F_{3LU} folds with rounded hinges and sub-horizontal axial planes (Fig. 5c). The A_{3LU} axes show a N-S trend and sub-horizontal plunge. At the outcrop scale the S_{3LU} foliation occurs as convergent fanning axial plane crenulation cleavage in the metapelites and metarenites whereas in the metalimestones it is represented by a disjunctive cleavage. The shear zones at the boundaries of the LU are deformed by the F_{3LU} folds.

At the microscale, the S_{3LU} foliation in metapelites is classifiable as crenulation cleavage (Figs. 5e and h) where the main deformation mechanism are pressure solution and reorientation of pre-existing tabular grains associated locally to minor recrystallization of Qz + Cal + Fe-oxides. Recrystallized calcite crystals show twins belonging to Type 1 of Burkhard (1992) classification that developed at T < 200°C.
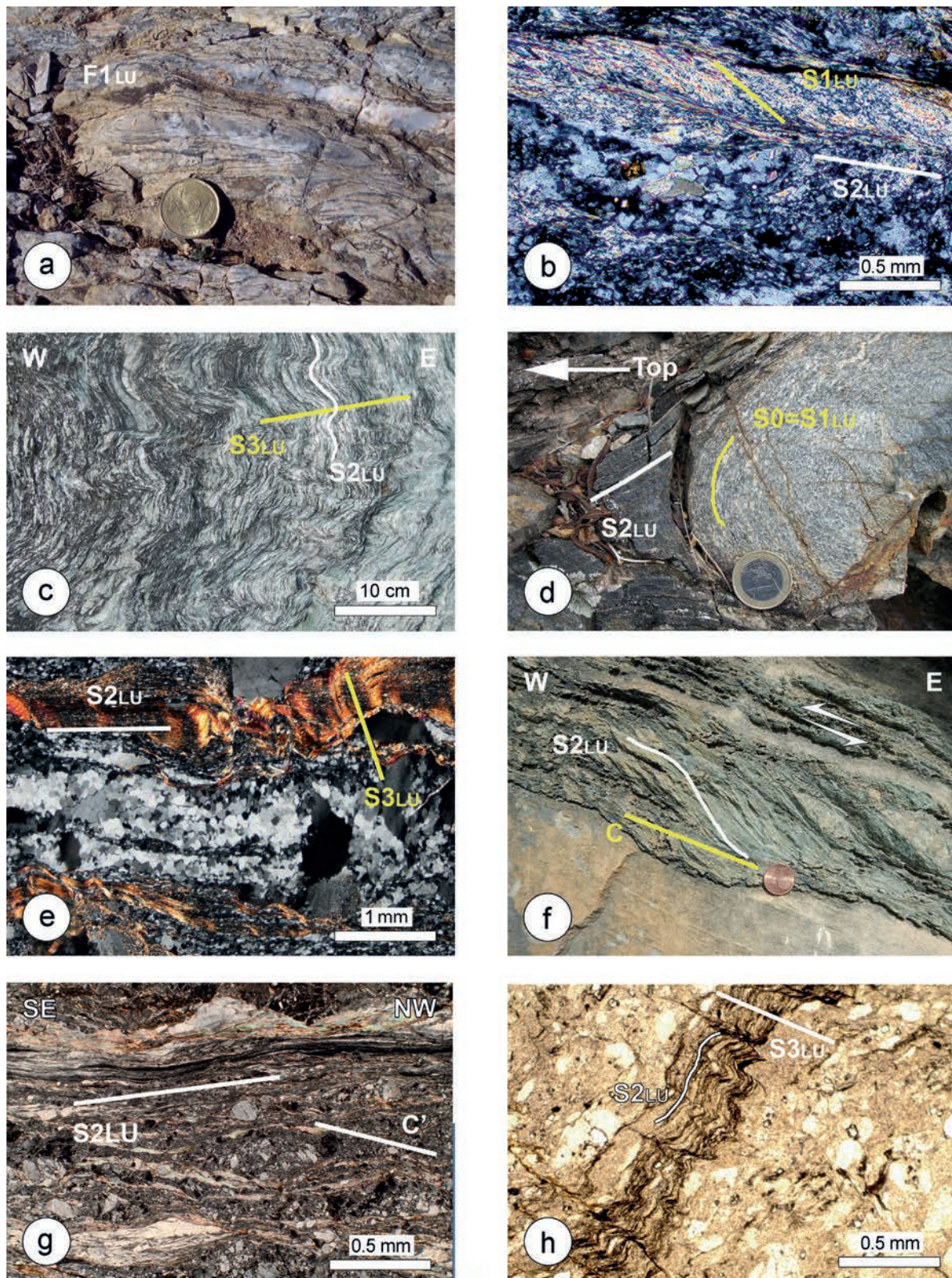
Fig. 5 - Meso- and microphotographs showing the polyphase deformation features of the Lower Units. a) F_{1LU} sheath fold in the Laminated Metalimestone Fm. of Piedigriggio-Prato Unit, Monte Cecu, area North of Corte (modified from Di Rosa et al., 2017a); b) S_{1LU}-S_{2LU} foliations interference pattern in the Metasandstone Fm., Castiglione-Popolasca Unit (sample CM29A) in the Francardo-Ponte Leccia area, crossed Nicols (modified from Di Rosa et al., 2020); c) S_{2LU}-S_{3LU} foliations interference pattern in the metagranitoids of Ghisoni Unit, Fium'Orbo Valley, area Vezzani Ghisoni; d) relationships between S_0/S_{1LU} and S_{2LU} foliations in the Metabreccia Fm. of Piedigriggio-Prato Unit, Bistuglio, area North of Corte (modified from Di Rosa et al., 2017b); e) Granoblastic layer consisting of recrystallized quartz affected by incipient recrystallization by subgrain rotation in the Ghisoni Unit metagranitoids, Vezzani-Ghisoni area, crossed Nicols (modified from Di Rosa et al., 2019b); f) S-C fabric related to the S_{2LU} foliation in the Metabreccia Fm. of Castiglione-Popolasca Unit, Restonica Valley, area South of Corte (modified from Di Rosa et al., 2020); g) S-C' microfabric in the Metavolcanics and Metavolcaniclastics Fm. of Ghisoni Unit, Vezzani-Ghisoni area; crossed Nicols (C': shear plane, modified from Di Rosa et al., 2019b); h) S_{2LU}-S_{3LU} foliations interference pattern in the Metasandstone Fm. of Piedigriggio-Prato Unit, area North of Corte, parallel Nicols (modified from Di Rosa et al., 2017a).

Schistes Lustrés Complex (SL)

The Inzecca-Lento Unit shows a complex structural setting resulting from a polyphase deformation history (Fig. 6), associated with development of a peak metamorphism under blueschist facies P-T conditions (Gibbons et al., 1986; Waters, 1990; Fournier et al., 1991; Caron, 1994; Daniel et al., 1996; Brunet et al., 2000; Martin et al., 2011; Vitale Brovarone et al., 2011; Vitale Brovarone and Herwartz, 2013; Rossetti et al., 2015).

D_{1SL} - Despite the strong transposition produced by the subsequent deformations (mainly D_{2SL} phase), evidences of the oldest deformation history at both meso- and micro-scale are still preserved in the low-strain domains of metabasalts, metagabbros and marble bodies. The meso-scale D_{1SL} structures are preserved in the marble layers as rare, generally rootless, intrafolial isoclinal folds (Fig. 7a), with acute hinge zones and strongly thinned limbs. No clear attitude

of the A_{1SL} axes can be determined, probably related to the non-cylindrical nature of F_{1SL} folds. An S_{1SL} continuous foliation, still well preserved in metagabbros and metabasalts is the most penetrative structural element of the phase, associated with a NE-SW trending L_{1SL} mineral/stretching lineation defined by prolate aggregates of Qz + Cal grains, as well as preferred orientation of HP mineral grains such as Na-Amp, Lws and Cr-rich Ph (Fig. 7b).

In metabasites, S_{1SL} foliation is preserved in the D_{2SL} microlithons as a continuous schistosity (Passchier and Trouw, 2005) marked by oriented elongated grains of Na-Amp + Ph + Qz + Ab in the metabasalts (Fig. 7c), and by Na-Amp + Lws + Ca-rich Ph and minor Qz oriented grains in the metagabbros. S_{1SL} continuous cleavage is only rarely visible in the micaschists of the Erbajolo Fm., where it is defined by a metamorphic mineral assemblage of Ph, Chl, Qz and Cal. In the calcschists the relic S_{1SL} foliation can be identified in the hinge zone of the F_{2SL} folds in the microlithons along the S_{2SL} foliation.

D_{2SL} - As in the other units of the SL, the S_{2SL} foliation in Inzecca-Lento Unit is the main planar anisotropy recognized at field-scale in micaschists and calcschists. S_{2SL} foliation is a continuous foliation frequently bearing shear sense indicators as σ-type tails around boudinated Qz veins. When restored from subsequent deformations, the attitude of the S_{2SL} foliation ranges from NE-SW in the northern areas to N-S and NW-SW in the southernmost one, whereas the sense of asymmetry of kinematic indicators point to a top-to-the NW sense of shear. In the metabasalts, metagabbros and marble, the S_{2SL} foliation is a crenulation cleavage. S_{2SL} is always parallel to the axial-plane of F_{2SL} isoclinal, cylindrical folds (Fig. 7d), with approximate similar geometry and subacute to rounded thickened hinges zones and stretched limbs with boudinage, necking and pinch-and-swell structures. The A_{2SL} axes trend ranges from NW-SE to NE-SW in the different areas, whereas the plunge is everywhere at low angle.

In thin sections S_{2SL} generally occurs as composite layering where the metamorphic minerals recrystallized during the D_{2SL} phase are superimposed on the pre-existing D_1 HP minerals. Only in the F_{2SL} hinge-zones, the S_{2SL} foliation occurs as a crenulation cleavage, characterized by smooth cleavage domains showing a gradational to discrete transition to the microlithons where the S_{1SL} foliation is visible (Fig. 7e). In the metabasalts, the D_{2SL} deformation is associated with recrystallization of Chl + Qz + Ab + Ca/Na-Amp + Ep and minor amount of Spn. The Ca/Na-Amp typically occurs as pseudomorphs on previous Na-Amp. In the metagabbros the S_{2SL} foliation is characterized by Qz ribbons and by the growth of Chl and Ph around the pre-existing HP minerals. In the meta-radiolarites the S_{2SL} foliation is classifiable as a disjunctive cleavage defined by white mica-rich layers separating microlithons of Qz grains. The Qz grains, characterized by a planar shape fabric, show evidences for complete dynamic recrystalization trough grain boundary migration and subgrain rotation processes (high irregular grain boundaries, gradual transition between subgrains and new grains of the same size). In the micaschists the S_{2SL} foliation is characterized by the development of Ph + Chl + Qz + Ab + Cal. In these lithotypes, the kinematic indicators, mainly σ-type porphyroclasts of Qz and Amp, suggest a top-to-the W sense of shear.

D_{3SL} - The phase includes F_{3SL} folds and associated spaced S_3 axial-plane foliation overprinting all D_{2LS} structural elements. In the metasedimentary rocks the F_{3SL} folds are
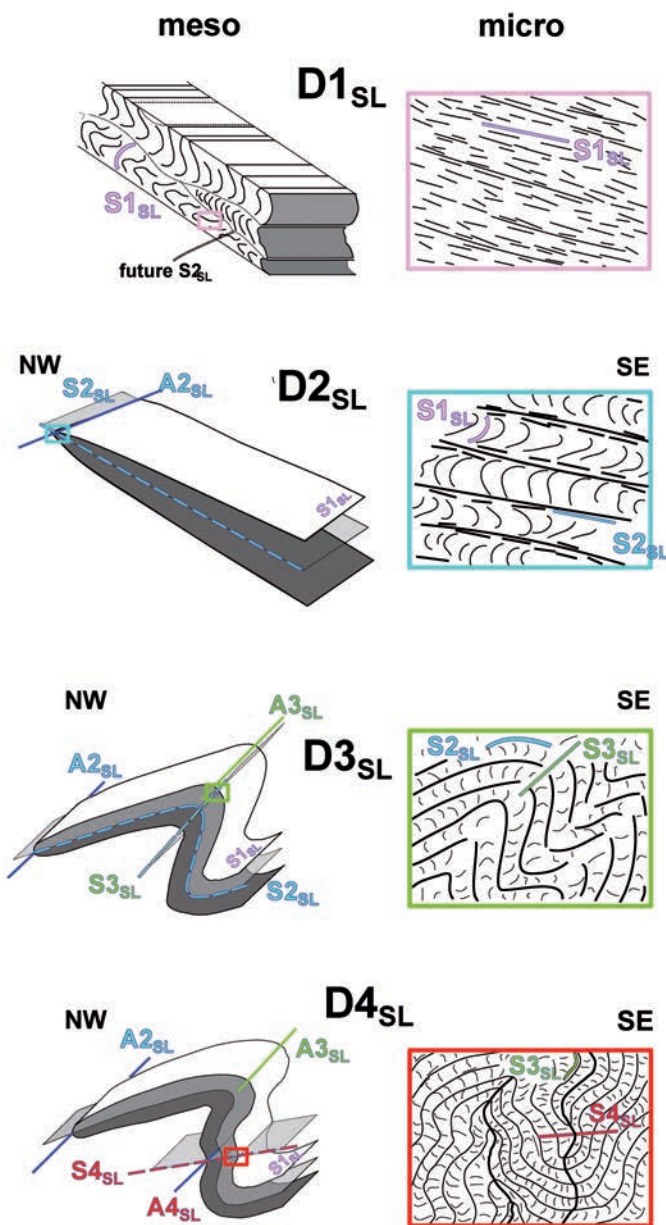

Fig. 6 - Sketches showing meso- and microscale deformation features in the Schistes Lustrés Complex.

close to open and show rounded hinge zones. They always display a marked asymmetric geometry showing an eastward vergence. The A_{3SL} axes trend about N-S with variable plunge angles, whereas AP_{3SL} axial planes are steeply inclined with predominately N-S strikes. Generally, the meso-scale F_{3SL} folds are associated with an S_{3SL} foliation, that can be classified as a crenulation cleavage in the micaschists and as disjunctive cleavage in the more competent lithotypes.

At the micro-scale the S_{3SL} foliation is recognized only in the micaschists from the Erbajolo Fm., and it can be classified as a crenulation cleavage with smooth cleavage domains and gradational transition to the microlithons. In the micaschists, the fabric is characterized by displacement-controlled strain fringes, developed around opaque minerals.

D_{4SL} - It produced gentle to open, long wavelength (up to several meters), parallel F_{4SL} folds, with sub-horizontal PA_{4SL} axial planes (Fig. 7f). Locally, some minor-scale kink-folds occur. The S_{4SL} foliation is a spaced disjunctive cleavage, generally well-developed exclusively in the hinge zone of the F_{4SL} folds. No metamorphic mineral assemblage related to D_{4SL} phase have been observed. Widespread low-angle shear
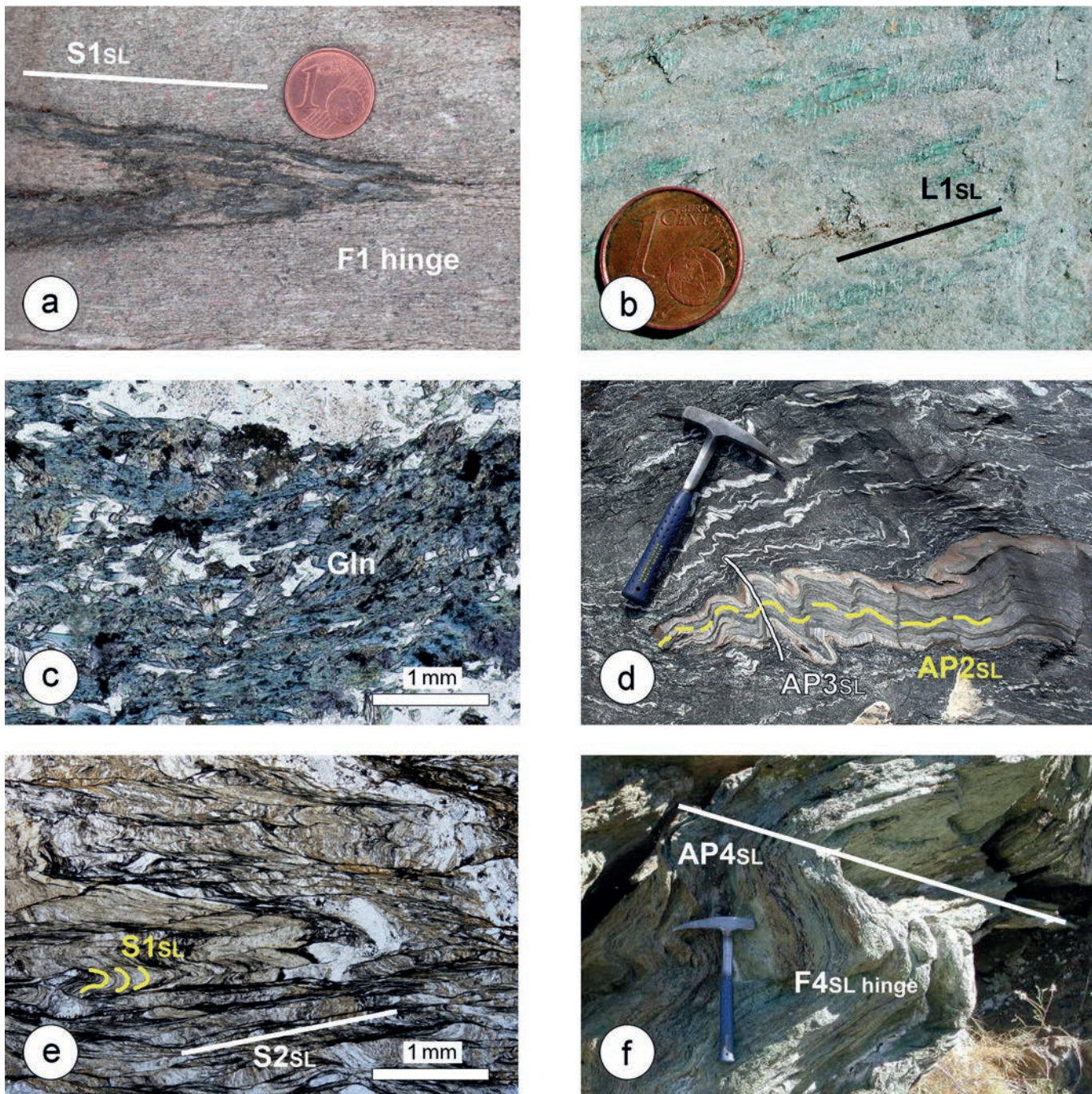
Fig. 7 - Meso- and micro-photographs showing the polyphase deformation of the Inzecca-Lento Unit, Schistes Lustrés Complex; a) F_1 fold in the Marble Fm., North Corte area; b) L_{1SL} mineral/stretching lineation of Cr-rich Ph in metagabbros; c) oriented grains of glaucophane (Gln) in the metagabbros; d) isoclinal F_{2SL} folds refolded by F_{3SL} folds. The axial planes AP_{2SL} and AP_{3SL} are indicated; e) relics of the S_{1SL} foliation within the S_{2SL} foliation in a pelitic layer in the calcschists,; f) F_{4SL} open folds, with sub-horizontal AP_{4SL} in axial plane.

zones are related to this phase and are characterized by S-C structures that, after restoration from subsequent deformations, display a normal fault motion with a top-to-the E sense of shear.

Upper Units (UU)

In both Balagne Nappe and Bas-Ostriconi Unit, we recognized a similar polyphase deformation history (Fig. 8), consisting of three distinct deformation phases, hereafter referred as D_{1UU}, D_{2UU}, D_{3UU} phases (Egal, 1992; Marroni and Pandolfi, 2003; Durand-Delga et al., 2005; Pandolfi et al., 2016).

D_{1UU} - No folds related to this phase have been identified in Bas-Ostriconi Unit (Pandolfi et al., 2016) whereas in the Balagne Nappe Egal (1992) and Marroni and Pandolfi (2003) have reported non-cylindrical, tight to isoclinal F_{1UU} folds characterized by an approximately similar geometry and by subrounded and thickened hinge zones (Fig. 9a). F_{1UU} axes trend from N-S to NW-SE with a northward plunge. In the field a pervasive S_{1UU} foliation parallel or at low angle with bedding (S_0) is widespread in both units. An LS_0-S_{1UU} intersection lineation is mainly represented by S_{1UU} foliation-S_0 intersections and mullion structures. Several Cal veins, with a thickness ranging from 2-3 mm to 6-7 cm, occur parallel

to the S_{1UU} foliation and S_0. Along the S_{1UU} foliation, well-developed asymmetric pressure shadows are found around Py crystals and detrital minerals, showing infillings of fibrous minerals such as Qz, phyllosilicates and Cal. After restoration from the subsequent deformation phases, these structures give a top-to-the W sense of shear. Cal and/or Qz fibres infilling pressure shadows around Py crystals are aligned to define a NW-SE trending L_{1UU} mineral lineation on the S_{1UU}.

In thin sections from metapelites and metasiltites samples, the S_{1UU} foliation (Fig. 9b) is a penetrative and continuous slaty cleavage characterized by elongated Qz + Ab + Cal + Ph aggregates surrounded by fine-grained, aligned recrystallized phyllosilicates (white mica, Chl and Stp). In the metalimestones the S_{1UU} foliation is characterized by a spaced disjunctive cleavage marked by pressure-solution.

D_{2UU} - This phase produced the most evident structures also in the UU, with a strong re-orientation of the S_0/S_{1UU} surface. The structures are mainly represented by asymmetric, tight to close F_{2UU} folds with sub-rounded to rounded hinge zones. The more competent layers are affected by boudinage along the F_{2UU} fold limbs and the fine-grained layers are interested by pinch and swell passive folds. The axial planes are steeply (50° to 80°) dipping whereas the A_{2UU} fold axes show a trend ranging from NW-SE to N-S. The asymmetry of the F_{2UU} folds, as detected also at map-scale, suggests a westward vergence. The F_{2UU} folds show a S_{2UU} foliation (Fig. 9c) everywhere parallel or subparallel to F_{2UU} fold axial planes. Generally, the S_{2UU} foliation is refracted at the boundary between the different layers, because of the strong viscosity contrast between the layers with different grain size. Fibrous, Cal veins at high angle to the S_0 generally developed during the D_{2UU} phase. Associated with this phase, are also low-angle thrusts responsible for internal imbrications in both Bas-Ostriconi Unit and Balagne Nappe. Kinematic indicators, such as S-C structures, reveal a top-to-the W sense of shear for these thrusts (Fig. 9d). In thin section, the S_{2UU} axial plane foliation developed in the shales and siltstones is a convergent fanning crenulation cleavage of zonal type (Fig. 9e), with parallel domains showing discrete transition. The crenulation cleavage is absent or poorly developed in limestones and sandstones. During the D_{2UU} phase, recrystallization of Qz and Cal occurred.

D_{3UU} - This phase produced gentle to open, asymmetric F_{3UU} folds with interlimb angles ranging from 80° to 130° (Fig. 9f). The A_{3UU} axes show a N-S trend, whereas the AP_{3UU} axial-planes are sub-horizontal or low-angle surfaces generally westward dipping. These folds, that generally display a clear eastward vergence, show an alternation of different fold classes along the same axial plane. In the F_{3UU} hinge zones, the S_{3UU} axial-plane foliation is represented by a spaced, disjunctive cleavage. During D_{3UU} phase, some of the thrust faults related to the D_{2UU} phase were reactivated as low-angle normal faults.

MINERAL CHEMISTRY AND P-T CONDITIONS

Metamorphic evolution and related P-T paths have been reconstructed only for the LU and SL, whereas in the UU the very low-grade imprint does not allow any P-T path determination. The study of the metamorphism associated with the LU and SL deformation history has been performed based on the relationships between the microstructures and the
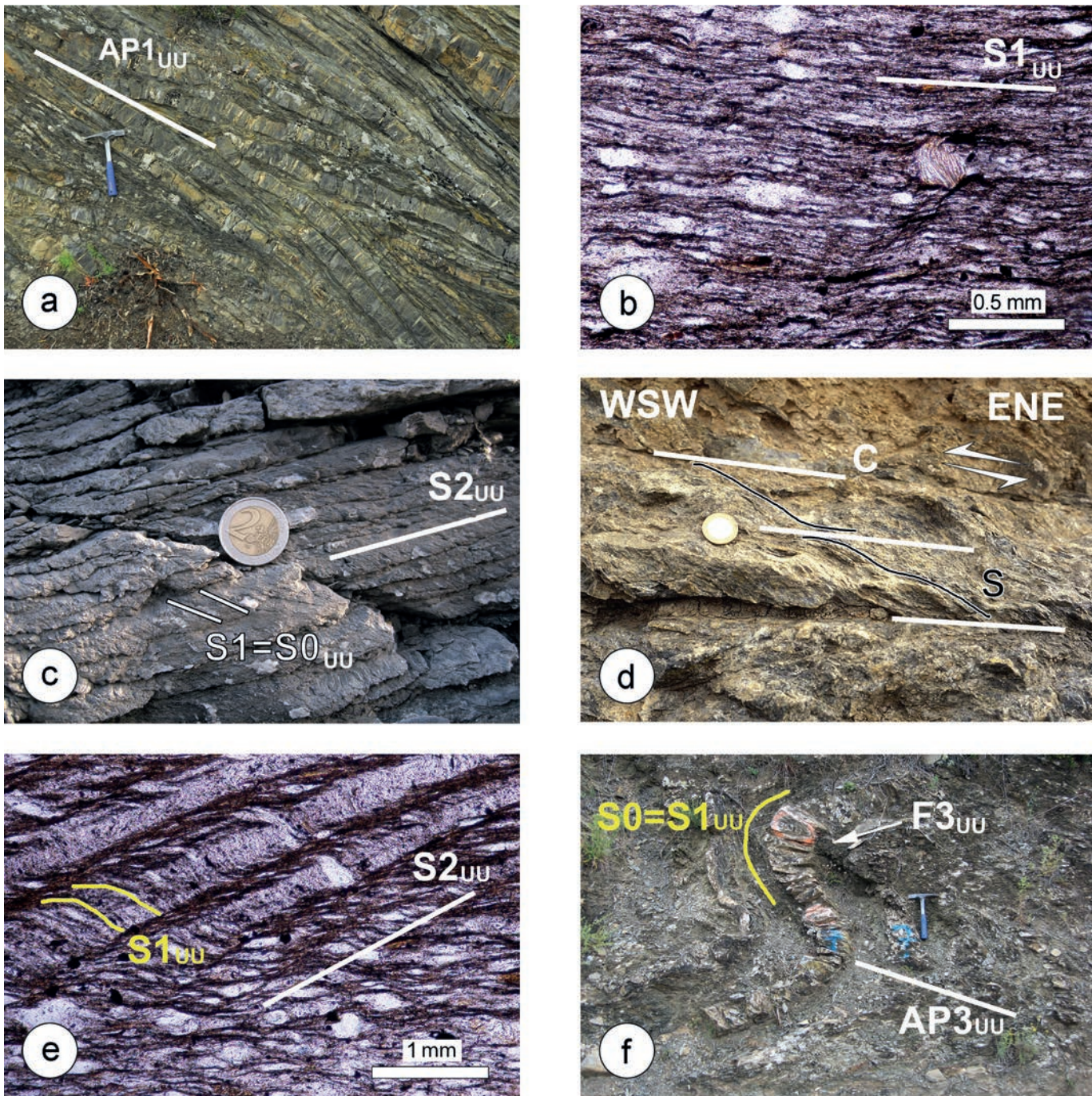

Fig. 8 - 2D sketches showing meso- and microscale deformation features in the Upper Units.

Fig. 9 - Meso- and micro-photographs showing the polyphase deformation of the Upper Units. a) D_{1UU} phase, isoclinal fold from Lydienne Flysch, Balagne Nappe. The axial plane ($AP1_{UU}$) is indicated. b) $S_1=S_{0UU}$ foliation in siltstones from Lydienne Flysch, Balagne Nappe. c) S_{1UU} and S_{2UU} foliation relationships in F_{2UU} hinge zone of the Narbinco Flysch, Bas-Ostriconi Unit; d) S-C structure developed along D_2 phase-related shear zone from San Martino Fm. Balagne Nappe. From Marroni and Pandolfi, 2003. e) photomicrograph showing S_{1UU} and S_{2UU} foliation relationships in the Lydienne Flysch, Balagne Nappe; f) F_{3UU} fold hinge zone in the San Martino Fm., Balagne Nappe. The axial plane (AP_{3UU}) and the composit S_0-S_{1UU} foliation are also indicated.

recrystallization of metamorphic parageneses in selected rock types. Quantitative and semi-quantitative methods have been applied in order to constrain the pressure (P) and temperature (T) ranges related to the equilibria of Na-Amp + Ph + Qz + Ab + Ep in meta-aplitic dykes and Chl + Ph + Ab + KFsp + Qz ± Cal in metapelites (Table 1).

The P-T conditions registered by the meta-aplitic dykes were characterized by Malasoma et al. (2006) using TWEEQ software (Berman, 1991). Regarding the metapelites, several methods were applied to estimate the P and T ranges given by the local equilibrium of Chl and Ph end-members within the microstructures (Di Rosa et al., 2017b; 2019b; 2019c; 2020). Chl-Ph couples grown in presence of Qz + Ab + K-Fsp + Cal within the same microstructure (i.e. in the same foliation) have been sampled in the metapelites of several tectonic units belonging to LU and SL, in order to reconstruct their P-T paths. The results obtained with the Chl-Qz-wt (Vidal et al., 2006), the Ph-Qz-wt (Dubacq et al., 2010) and the Chl-Ph-Qz-wt (Vidal and Parra, 2000) quantitative methods were compared with those gained by classical geobarometry (Massonne and Schreyer, 1987) and geothermometry (Cathelineau and Nieva, 1985; Cathelineau, 1988; Lanari et al., 2014).

Table 1 - Summary of the P-T conditions included in this work.

	Localitiy	Tectonic unit	Lithotypes	sample	Results	Methods	Reference
North Balagne	Bocca di Fuata	VBS (LU)	Meta-arenite	BV2	**D1$_{LU}$ (peak):** 0.6 ± 0.15 GPa, 325 ± 20°C; **D2$_{LU}$:** 0.35 ± 0.06 GPa, 315 ± 20°C	Chl-Ph-Qz-wt	Malasoma & Marroni, 2007
Ponte Leccia/ Francardo	Castiglione	CPU (LU)	Metabreccia Fm.	CM29A	**Early D1$_{LU}$:** 1. 10-0.75 ± 0.20 GPa, 250-330 ± 30°C; **Late D1$_{LU}$:** 0.65-0.50 ± 0.20 GPa, 320-345 ± 30°C; **D2$_{LU}$:** 0.45-0.25 ± 0.20 GPa, 310-250 ± 30°C	Chl-Qz-wt; Ph-Qz-wt; Chl-Ph-Qz-wt; Massonne & Schreyer (1987); Cathelineau & Nieva (1985)	Di Rosa et al., 2019a
	Prato di Giovellina	CAU (LU)	Aplite dyke in metagranitoid	PC105	**D1$_{LU}$:** 0.80-0.50 ± 0.20 GPa, 300-370°C	Berman (1991)	Malasoma et al., 2006
North Corte	Bocca Ominanda	PPU (LU)	Metabreccia Fm.	CM32C	**Early D1$_{LU}$:** 1.10-1.00 ± 0.20 GPa, 250-270 ± 30°C; **Late D1$_{LU}$:** 0.80-0.65 ± 0.20 GPa, 280-390 ± 30°C; **D2$_{LU}$:** 0.45-0.25 ± 0.20 GPa, 270-230 ± 30°C	Chl-Qz-wt; Ph-Qz-wt; Chl-Ph-Qz-wt; Massonne & Schreyer (1987); Cathelineau (1988)	Di Rosa et al., 2017a
	Monte Cecu	PPU (LU)	Metabreccia Fm.	CM21	**Early D1$_{LU}$:** 1.05-0.75 ± 0.20 GPa, 200-240 ± 30°C; **Late D1$_{LU}$:** 0.80-0.50 ± 0.20 GPa, 340-400 ± 30°C; **D2$_{LU}$:** 0.40-0.25 ± 0.20 GPa, 300-240 ± 30°C	Chl-Qz-wt; Ph-Qz-wt; Chl-Ph-Qz-wt; Massonne & Schreyer (1987); Lanari et al., (2014)	Di Rosa et al., 2017a
	Golo Valley	CAU (LU)	Metagranitoid	CM40	**Peak T conditions:** ca. 300-400°C	Stipp et al. (2002); Passchier and Trouw (2005)	Di Rosa et al., 2017b
	Buttinacce	IZU-Buttinacce (SL)	Calcshist	CMD121B	**D1$_{SL}$:** 0.55-0. 65 ± 0.20 GPa, 265-310 ± 30°C; **D2$_{SL}$ (peak):** 0.85-0.70 ± 0.20 GPa, 240-275 ± 30°C; **Late D2$_{SL}$:** 0.60-0.40 ± 0.20 GPa, 200-275 ± 30°C	Chl-Qz-wt; Ph-Qz-wt; Chl-Ph-Qz-wt; Massonne & Schreyer (1987); Lanari et al., (2014)	Di Rosa et al., 2020
South Corte	Tavignano Valley	CPU (LU)	Metabreccia Fm.	CM22B	**Early D1$_{LU}$:** 1.20-1.10 ± 0.20 GPa, 250-330 ± 30°C; **Late D1$_{LU}$:** 0.80-0.55 ± 0.20 GPa, 320-350 ± 30°C; **D2$_{LU}$:** 0.35-0.25 ± 0.20 GPa, 310-230 ± 30°C	Chl-Qz-wt; Ph-Qz-wt; Chl-Ph-Qz-wt; Massonne & Schreyer (1987); Lanari et al., (2014)	Di Rosa et al., 2019a
	Botro	IZU-Botro (SL)	Calcschist	CMD118	**D1$_{SL}$:** 0.75-0.65 ± 0.20 GPa, 220-245 ± 30°C; **D2$_{SL}$ (peak):** 1.00-0.85 ± 0.20 GPa, 200-250 ± 30°C; **Late D2$_{SL}$:** 0.60-0.50 ± 0.20 GPa, 150-190 ± 30°C	Chl-Qz-wt; Ph-Qz-wt; Chl-Ph-Qz-wt; Massonne & Schreyer (1987); Cathelineau & Nieva (1985)	Di Rosa et al., 2020
Vezzani/ Ghisoni	Fium'Orbo Valley	GHU (LU)	Metavolcanic and Metavolcaniclastic Fm.	CMD50D	**Early D1$_{LU}$:** 0.81-0.72 ± 0.20 GPa, 245-250 ± 30°C; **Late D1$_{LU}$:** 0.68-0.39 ± 0.20 GPa, 263-243 ± 30°C; **D2$_{LU}$:** 0.37-0.13 ± 0.20 GPa, 228-209 ± 30°C	Chl-Qz-wt; Ph-Qz-wt; Chl-Ph-Qz-wt; Massonne & Schreyer (1987); Lanari et al., (2014)	Di Rosa et al., 2019a
	Fium'Orbo Valley	GHU (LU)	Metagranitoid	CMD37	**Peak T conditions:** ca. 300-400°C	Stipp et al. (2002); Passchier and Trouw (2005)	Di Rosa et al., 2019a

We summarize here the main results of these studies distinguishing those obtained for continental (i.e. LU) and oceanic units (i.e. SL). Detailed descriptions of the employed methodologies are reported in Malasoma et al. (2006) and Di Rosa et al. (2020 and reference therein) and the main results are reported in Tables 1-2-1S and Figs. 10 and 11.

Lower Units (LU)

Determination of the P-T equilibration conditions for the LU located along the boundary between Hercynian and Alpine Corsica have been the object of several studies in the last two decades (Malasoma et al., 2006; Malasoma and Marroni, 2007; Di Rosa et al., 2017b; 2019b; 2020). The metamorphic evolution of the Volparone Breccia Slice (North Balagne area), Castiglione-Popolasca and Piedigriggio-Prato Units (from Ponte Leccia to South Corte) and Ghisoni Unit (Vezzani-Ghisoni) was reconstructed through the study of the metapelites (Malasoma and Marroni, 2007; Di Rosa et al., 2017b; 2019b; 2020), whereas the P-T conditions for the Croce d'Arbitro Unit (from Ponte Leccia to North Corte areas) were based on the estimates obtained for the meta-aplitic dykes (Malasoma et al., 2006).

The metapelites studied in the Ghisoni Unit belong to the Permian Metavolcanic and Metavolcaniclastic Fm., whereas those chosen for Castiglione-Popolasca and Piedigriggio-Prato Units as well as for Volparone Breccia Slice belong to the Metabreccia and Metarenite Fms. attributed to the middle-late Eocene. In all the investigated samples two foliations (S_{1LU} and S_{2LU}), with associated the recrystallization of Chl + Ph + Ab + KFsp + Qz ± Cal, have been distinguished.

Di Rosa et al. (2020 and reference therein) observed that the analyzed Chl and Ph related to the S_{1LU} foliation of Castiglione-Popolasca, Piedigriggio-Prato and Ghisoni Units are characterized by different compositions which have been interpreted as two distinct generations. A third generation of Chl and Ph has been identified as growing along the S_{2LU} foliation. The compositional characterization of the different Chl + Ph generations are summarized:

– **first Chl-Ph generation (early S_{1LU} foliation)** - Chl have high Si and low Al ranging between 2.70-3.00 apfu (atom per formula unit) and 2.20-2.75 apfu, respectively; only small differences between each single sample are observed (Fig. 10, Table 2). MgO + FeO content in Chl is always < 40%. Chl composition is intermediate between Clc + Dph and Ame end-members due to wide scatter of SiO_2 contents. Ph of the first generation are characterized by the highest Si content (3.30-3.70 apfu) and Al_2O_3 percentage lower than 60% in all the samples. Given the Al depletion, the Ph composition approaches the Cel end-member;

– **second Chl-Ph generation (late S_{1LU} foliation)** - Chl have a more variable composition than those of the first generation and tends to get depleted in Si (2.55-3.00 apfu). The low SiO_2 contents make the composition of the Chl of this generation closer to the Ame end-member. Ph are characterized by Si intermediated between those of the first and the third generations (3.30-3.55 apfu, Fig. 10). The Al content of Ph is higher than those of the first generation, leading to compositions intermediate between Cel and Mus end-members;

– **third Chl-Ph generation (S_{2LU} foliation)** - Chl are characterized by Si content similar to that of the first generation (from 2.80 to 3.00 apfu) but higher Al content (from 2.30 to 3.00 apfu) which leads them to approach the pure Sud composition. Ph of the third generation are depleted in Si

(from 3.00 to 3.60 apfu) and enriched in Al. Their composition is intermediate between Mus and Prl end-members.

The results obtained with the above-referenced methods (Table 2) allowed estimating the P-T conditions for the LU. The highest P conditions (1.20-1.10 GPa) are registered by Castiglione-Popolasca Unit during the early D_{1LU}. Lower pressure conditions (0.55-0.80 GPa) were registered by Castiglione-Popolasca Unit during the T peak (320-350°C) in the late D_{1LU} phase. On the other hand, the highest T conditions of 340-400°C are reached in association to a pressure range of 0.50-0.80 GPa by the Piedigriggio-Prato Unit during the late D_{1LU} phase. Two different trends are followed by the LU: an "isothermic" path (e.g., Castiglione-Popolasca and Ghisoni units), in which the increase of temperature during the exhumation path is less than 100°C, and a "warm" path (e.g., Piedigriggio-Prato Unit) in which the temperature between the P- and the T-peaks increases of at least 150°C, causing the T peak to be reached during the late D_{1LU} phase between 300 and 400°C. Despite the differences related to the D_{1LU} phase, all the samples registered the D_{2LU} phase (i.e. associated with the P-T equilibrium conditions of the third Chl-Ph generations) at lower pressure and temperatures.

The P-T conditions of Castiglione-Popolasca Unit have been also constrained through the association Na-Amp + Ph + Qz + Ab + Ep found in a meta-aplitic dyke in the Ponte Leccia/Francardo area (Malasoma et al., 2006). The metamorphic peak conditions, calculated using the TWEEQ sofware (Berman, 1991), gives a P range between 0.50 and 0.80 GPa associated with a T range of 300-700°C (Fig.11, Tables 1-2).

Schistes Lustrés Complex (SL)

The metamorphic conditions of Inzecca-Lento Unit has been estimated in the metapelites layers of the Erbajolo Fm. from the SL of the Corte slices (SL Corte slices) cropping out in the areas North and South of Corte (Di Rosa et al., 2020). The calcschists of the Erbajolo Fm. are characterized by two foliations (S_{1SL} and S_{2SL}) with the same mineralogical paragenesis of Chl + Ph + Qz ± Pl. Based on the Chl- and Ph- end-members proportion, three generations of Chl and Ph have been identified (Fig. 10): an old generation grown along the S_{1SL} foliation and two different generations aligned along the S_{2SL} foliation (Tables 1-2 and Fig. 11):

– **first Chl-Ph generation (S_{1SL} foliation)** - Chl show Si content varying from 2.55 to 2.90 apfu with the highest values for the sample CMD121B, which is depleted in Al compared to the CMD118 (Fig. 10, Tab. 2). Based on the SiO_2 content lower than 30% in both samples, the composition of the Chl of the first generation is close to the Ame end-member. Ph have a Si content between 3.20 to 3.40 apfu whereas the K content is different in the two samples (0.50-0.90 apfu in CMD118 and 0.75-0-85 apfu in CMD121B). The composition of the first Ph generation is intermediate between Ms and Cel;

– **second Chl-Ph generation (early S_{2SL} foliation)** - Chl show higher Si (2.70-3.00 apfu) and lower Al (2.20-2.80 apfu) contents than those of the first generation. Lower percentage of MgO + FeO than those of the first generation moves the composition of the Chl of the second generation toward the Sud end-member. In the Ph, the Si content ranges between 3.15 and 3.45 apfu, whereas the K content is similar to those of the first generation. The MgO + FeO percentage is always higher than 20% and ranges from Ms end-member to a composition closer to the Cel end-member;
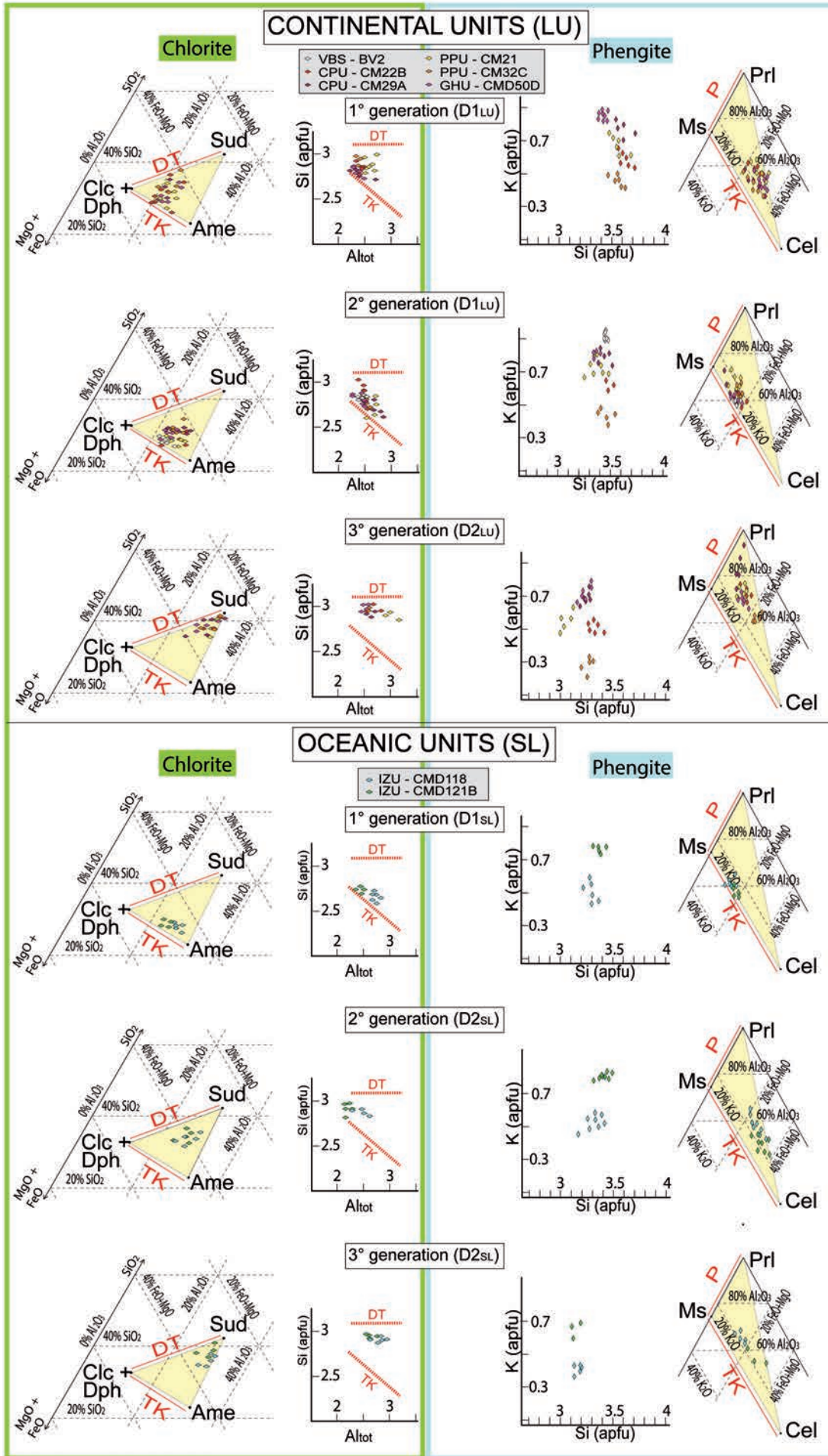
Fig. 10 - Binary and ternary diagrams showing Chl and Ph compositions of the metapelites studied by Malasoma and Marroni (2007) and Di Rosa et al. (2017b; 2019b; 2020). Each symbol in the diagrams represents the average value calculated on 15 spot analysis. Diagrams are related to the Chl (left column) and Phg (right column) analyses, respectively. The position of the DT (di-trioctahedral) and TK (Tschermak) substitutions in the Al/Si diagram are calculated by Trincal and Lanari (2016). Yellow triangles in the ternary diagrams are drawn following Vidal and Parra (2000). Malasoma and Marroni (2007) did not assign Chl and Ph from the sample BV2 (Volparone Breccia Slice) to a specific generation. Taking into account the different techniques employed by Malasoma and Marroni (2007) compared to those of Di Rosa et al. (2017b; 2019b; 2020), and thus assuming that the first generation has not been identified by Malasoma and Marroni (2007), we have chosen to insert the data related to Volparone Breccia Slice in the diagrams of the second generation because they show similar values to those of the other units.
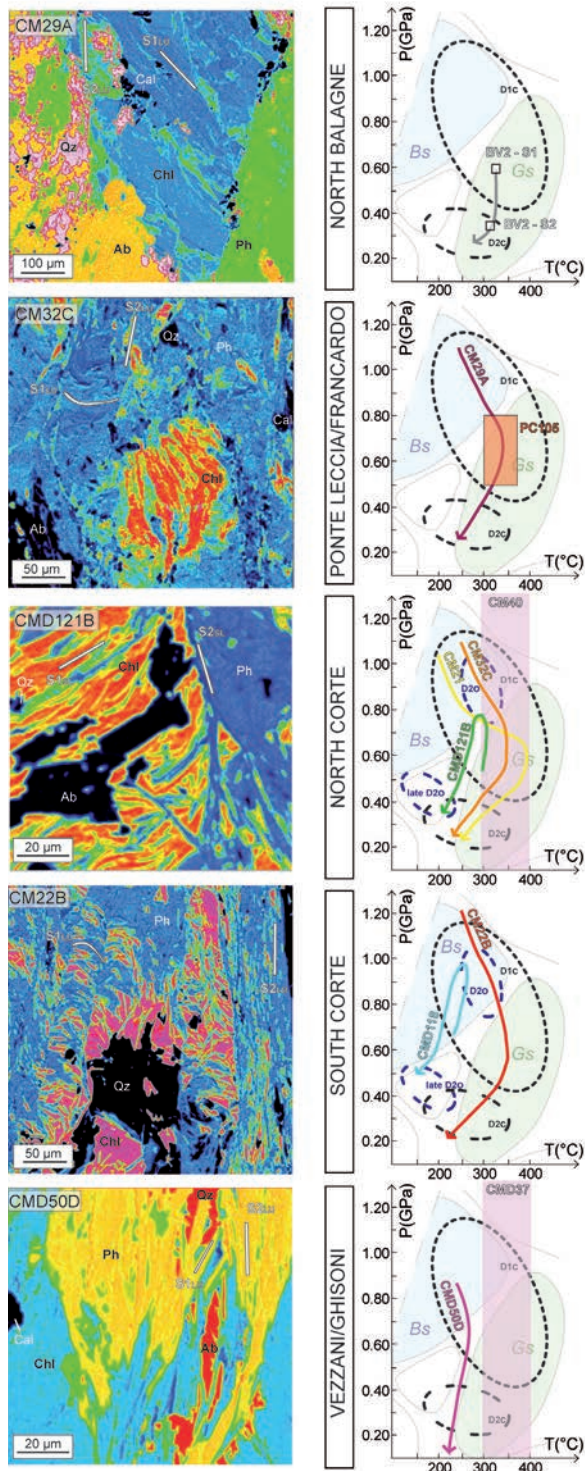
Fig. 11 - Examples of elemental maps acquired with EPMA (colors represent the intensities of a selected element: Si for CM29A and CMD50D, Mg for CM32C, CMD121B and CM22B) and P-T paths of samples from the five study areas and related formations (Volparone Breccia Slice, Castiglione-Popolasca Unit, Piedigriggio-Prato Unit, Ghisoni Unit, IZU-Buttinacce and IZU-Botro; modified after Malasoma et al., 2006; Malasoma and Marroni, 2007 and Di Rosa et al., 2019b; 2020). The paths (colored arrows) were drawn considering the best fit between the Chl-Qz-wt (Vidal et al., 2006), Ph-Qz-wt (Dubacq et al., 2010) and Chl-Ph-Qz-wt (Vidal and Parra, 2000) methods. White boxes in the P-T diagram of North Balagne (sample BV2) indicate the stability fields calculated by Malasoma and Marroni (2007). Orange box in the P-T diagram of Ponte Leccia/Francardo (sample PC105) indicate the P-T range of equilibrium calculated for a meta-aplitic dyke by Malasoma et al. (2006). Pink boxes represent the T range estimated for Croce d'Arbitro Unit (sample CM40) and Ghisoni Unit (sample CMD37) estimated for metagranitoids by Di Rosa et al., (2017a; 2019b).

– **third Chl-Ph generation (late S_{2SL} foliation)** - Chl show homogeneous composition in the two samples with Al ranging between 2.45 and 2.95 apfu and Si between 2.80 and 2.95 apfu (Fig. 10, Tab. 2). The depletion in MgO + FeO leads the composition of the third generation of Chl close to the pure Sud. Ph of the third generation have Si between 3.05-3.30 apfu, whereas the K content is slightly lower than those of the older generations. Considering the oxide abundances of the third Ph generation (ca. 20% MgO + FeO, 60% Al_2O_3 and 20% K_2O), the composition is intermediate between the three end-members.

The P-T conditions estimated for the SL (see Table 2) suggests that during the D_{1SL} phase, the Chl-Ph couples from both SL Corte slices are in equilibrium at similar P conditions of ca. 0.70-0.50 GPa but at different T conditions (220-245°C for IZU-Botro, South Corte and 265-310°C for IZU-Buttinacce, North Corte). During the D_{2SL} phase the P-T conditions range from 0.70 to 1.00 GPa and from 200-270°C in both slices. The P conditions registered by the third generation of Chl-Ph in the late D_{2SL} phase are similar in the two areas (0.50-0.60 GPa), but are associated with different T, i.e. 150-190°C for IZU-Botro, South Corte and 200-275°C for IZU-Buttinacce, North Corte (Table 2).

RECONSTRUCTION OF THE TECTONIC RELATIONSHIPS BETWEEN THE OCEANIC AND CONTINENTAL UNITS ALONG THE WESTERN EDGE OF ALPINE CORSICA

The relationships between the continental and oceanic units of Alpine Corsica are commonly described in literature as a simple thrusting of the SL and UU ensemble over the LU, with each unit characterized by an internal polyphase deformation acquired before the stacking (Durand-Delga, 1984; Gibbons and Horak, 1984; Bezert and Caby, 1988; Egal, 1992; Daniel et al., 1996; Marroni and Pandolfi, 2003; Malasoma et al., 2006; Garfagnoli et al., 2009). The boundaries among the units are east-dipping shear zones, with top-to-the W sense of shear, except in areas where they have been partly obscured due to the reworking by the CCSZ.

The more recent studies, that are the object of this review paper, have revealed a more complex setting, where the SL (and UU) not only overthrust on top of the LU, but they are also intricately imbricated with them. Object of this chapter is a description of the tectonic and map-scale relationships between the continental and oceanic units in the five study areas with reference to the deformation history described before.

North Balagne area
The western side of the North Balagne area is characterized by thrusting of the units stack westwards, onto the Hercynian Corsica (Fig. 12). Particularly, the UU lie on top of an imbricate stack of slices, that include small, elongated bodies of UU themselves (referable to the Balagne Nappe and Bas-Ostriconi Unit), and slices of LU that are imbricated with the Annunciata Unit (Cf. Palasca Unit after Nardi et al., 1978). The Annunciata Unit is a slice detached from the sedimentary cover of the Hercynian Corsica (Nardi et al., 1978; Durand-Delga, 1984) and made of well-bedded, siliciclastic turbidites of middle Eocene age (Annunciata Formation; Durand-Delga, 1984). The whole stack is folded in a large-scale, open, north-south trending synform (Marroni and Pandolfi, 2003). To the east this broad-scale structure is bounded by the CCSZ (Waters, 1990; Lacombe and Jolivet, 2005) that separates the North Balagne area from the Tenda Massif.
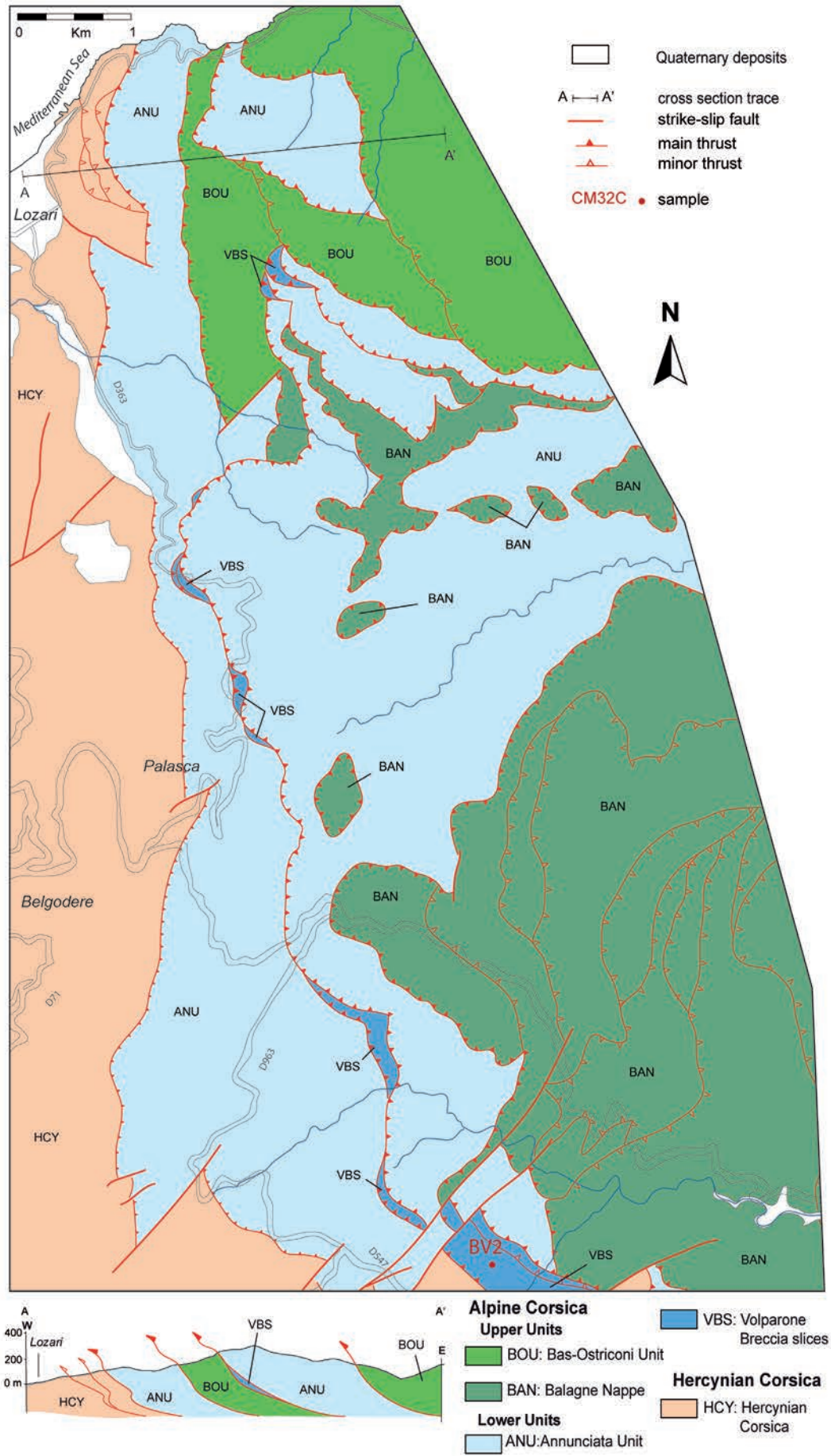
Table 2 - Representative electron microprobe analyses of the Cl-Ph pairs selected in the samples of metapelites.

Lower Units

	P-T estimates (Vidal and Parra. 2000)						T range (Vidal et al., 2006)			P range (Dubacq et al., 2010)			T max	Lowest P conditions related to the P-peak [Massonne and Schreyer. 1987]
	$D1_{LU}$ PHASE				$D2_{LU}$ PHASE									
	Early $D1_{LU}$ Chl-Ph		Late $D1_{LU}$ Chl-Ph		$D2_{LU}$ Chl-Ph		Early $D1_U$ Chl	Late $D1_{LU}$ Chl	$D2_{LU}$ Chl	Early $D1_{LU}$ Ph	Late $D1_{LU}$ Ph	$D2_{LU}$ Ph		
	T (°C)	P (GPa)	T (°C)	P (GPa)	T (°C)	P (GPa)	T (°C)	T (°C)	T (°C)	P (GPa)	P (GPa)	P (GPa)	T (°C)	P (GPa)
CM22B (CPU)	250-330	1.20-1.10	320-350	0.80-0.55	230-310	0.35-0.25	250-310	320-350	230-310	1.20-1.05	0.85-0.50	0.35-0.25	350 (Lanari et al.. 2014a)	1.25
CM29A (CPU)	250-330	1.10-0.75	320-345	0.65-0.50	250-310	0.45-0.25	250-300	315-340	260-320	1.10-0.80	0.5-0.65	0.30-0.50	320 (Cathelineau and Nieva. 1985)	1.30
CM21 (PPU)	200-240	1.05-0.75	340-400	0.80-0.50	240-300	0.40-0.25	200-235	350-385	195-230	1.00-0.80	0.55-0.80	0.35-0.40	345 (Lanari et al.. 2014a)	1.20
CM32 (PPU)	250-270	1.10-1.00	280-390	0.80-0.65	230-270	0.45-0.25	250-300	300-370	225-270	1.10-1.00	0.70-0.85	0.30-0.45	320 (Cathelineau. 1988)	1.26
CMD50D (GHU)	245-250	0.81-0.72	243-263	0.68-0.39	228-209	0.37-0.13	240-250	230-270	225-220	0.90-0.75	0.45-0.75	0.40-0.10	272 (Lanari et al.. 2014)	0.92

Schistes Lustrés Complex

	P-T estimates (Vidal and Parra. 2000)						T range (Vidal et al., 2006)			P range (Dubacq et al., 2010)			T max	Lowest P conditions related to the P-peak [Massonne and Schreyer. 1987]
	$D1_{SL}$ PHASE		$D2_{SL}$ PHASE											
	$D1_{SL}$ Chl-Ph		$D2_{SL}$ Chl-Ph		Late $D2_{SL}$ Chl-Ph		$D1_{SL}$ Chl-	$D2_{SL}$ Chl-	Late $D2_{SL}$ Chl	$D1_{SL}$ Ph	$D2_{SL}$ Ph	Late $D2_{SL}$ Ph		
	T (°C)	P (GPa)	T (°C)	P (GPa)	T (°C)	P (GPa)	T (°C)	T (°C)	T (°C)	P (GPa)	P (GPa)	P (GPa)	T (°C)	P (GPa)
CMD118 (IZU-Botro)	220-245-	0.65-0.75	200-250	1.00-0.85	150-190	0.60-0.50	220-240	205-240	150-175	0.60-0.75	1.00-0.90	0.50-0.60	340 (Cathelineau and Nieva. 1985)	1.10
CMD121A (IZU-Buttinacce)	270-290	0.50-0.70	245-300	0.90-0.75	140-215	0.50-0.45	275-305	250-310	160-200	0.55-0.70	0.75-0.90	0.45-0.65	335 (Lanari et al. 2014a)	1.15
CMD121B (IZU-Buttinacce)	265-310	0.55-0.65	240-275	0.85-0.70	200-275	0.60-0.40	265-320	220-280	200-270	0.45-0.60	0.85-0.65	0.60-0.40	325 (Lanari et al. 2014a)	1.0

Fig. 12 - Structural sketch of the North Balagne area and related cross section.

Ponte Leccia-Francardo area

In this area (Fig. 13) the LU crop out as a north-south trending stack with Castiglione-Popolasca Unit at the bottom and Croce d'Arbitro and Piedigriggio-Prato units at the top of the pile. These units overthrust the Hercynian Corsica in the west, whereas to the east they are topped by two oceanic units, the HP Inzecca-Lento (SL) and the Serra Debbione-Pineto Units (UU). A unique finding in this area is the occurrence of thin slices of metaserpentinites, derived from SL units, tectonically sandwiched in the Piedigriggio-Prato Unit, toward the top of the unit stack (Malasoma et al., 2006; 2020). All the unit boundaries are represented by west-verging, east-dipping ductile shear zones, that are folded together by east-verging folds. These folds locally rotate these units up to the vertical or, as in Castirla and Castiglione areas, overturn them. Subsequently, the relationships among the different units are modified by the brittle tectonics connected to the CCSZ. Along the Golo Valley, the relationships among LU and SL and the structures of the CCSZ are sealed by the late Burdigalian to Langhian marine and continental deposits of the Francardo Basin (Alessandri et al., 1977).

North Corte area

North Corte area (Fig. 14) is occupied by a continental stack comprising Castiglione-Popolasca, Croce d'Arbitro and Piedigriggio-Prato units on top, that were first mapped and named here as "Ecailles de Corte" (Durand-Delga 1984). They are emplaced over the Hercynian Corsica to the west and, in turn, are overthrust by the SL to the east. Although the SL units are referable to the Inzecca-Lento Unit (IZU), as elsewhere in the western edge of Alpine Corsica, the peculiarity of this area is the occurrence of intensely deformed slices of SL tectonically imbricated along the boundaries between the different LU (Di Rosa et al., 2017a; 2020); in the North Corte area, such slices are referred to as IZU-Buttinacce (Di Rosa et al., 2020).

South Corte area

In the South Corte area (Fig. 15) the SL occurs at the top of the LU by a high angle-shear zone, largely reworked by the CCSZ, and are represented by the Bagliacone-Riventosa Unit. The LU here comprise the southernmost portion of Castiglione-Popolasca Unit that overthusts to the west the Hercynian Corsica. The Castiglione-Popolasca Unit crops out as a series of thin slices with a steep or vertical attitude, probably as a consequence of the later deformation connected with CCSZ. Slices of the SL referable to the Inzecca-Lento Unit, and thus named IZU-Botro (Di Rosa et al., 2020), occur tectonically sandwiched between Castiglione-Popolasca Unit at the bottom and Bagliacone-Riventosa Unit on top.

Vezzani-Ghisoni area

In this area (Fig. 16) the LU, represented by Ghisoni Unit, are sandwiched between the Hercynian Corsica and the Inzecca-Lento Unit (SL) by high angle west-verging thrusts that are deformed by weak folds with low-angle axial plane and then are strongly overprinted by brittle deformation related to the CCSZ (Fig. 16b).

Therefore, it is shown that locally, e.g., north of Corte and in the Ponte Leccia-Francardo area, high-grade metamorphic oceanic units such as Inzecca-Lento Unit are tectonically sliced within high-grade units of continental affinity. In the northernmost area, i.e. North Balagne area, the continental units of the LU are tectonically sandwiched between the low-grade oceanic units of the UU, in an imbricated stack that involves slices of the sedimentary cover of the Hercynian Corsica. The North Balagne area demonstrates that the coupling between the oceanic and continental units may occur at shallow structural levels and involves not only the LU, but also the UU and the sedimentary cover of the Hercynian Corsica. Overall, the different areas provide a picture of the coupling between the oceanic and continental units at different structural levels.

Moving from north to south along the western edge of Alpine Corsica, we can observe the coupling between the oceanic and continental units at different structural levels. For the deeper structural levels, an imbrication occurred where the oceanic rocks were sliced and juxtaposed with and within the continental units. Moreover, the field data compiled in this review from our field mapping and data from literature (Bezert and Caby, 1988; Egal and Caron, 1988; Egal, 1992; Tribuzio and Giacomini, 2002; Molli and Tribuzio, 2004; Molli et al., 2006; Malasoma et al., 2006; Malasoma and Marroni, 2007; Di Rosa et al., 2017a; 2017b; 2019b; 2019c) allow defining time constraints for this tectonic slicing. There is general agreement that the coupling between the oceanic and continental units occurred during the late stage of the D_{2LU} and before the D_{3LU} folding phase that deforms all the tectonic boundaries among the units from Alpine Corsica. This D_{3LU} phase corresponds to the D_{3UU} and the D_{4SL} phases. In fact, slicing is constrained between the age of the youngermost deposits involved in the deformation, i.e. the late Eocene (Bartonian) Metasandstone Fm. found at the top of the LU succession (Bezert and Caby, 1988) and the onset of the sedimentation in the Francardo Basin (Ferrandini et al., 2003), whose base has been assigned to the Burdigalian (Alessandri et al., 1977). Therefore, the tectonic slicing between oceanic and continental units can be bracketed between 37.8 Ma, i.e. the age of the top of the Metasandstone Fm. (Bezert and Caby, 1988), and 20.4 Ma, i.e. the age of the base of the deposits of Francardo Basin (Alessandri et al., 1977). The whole deformation history of the LU, from the D_{1LU} to the $D_{3\ LU}$ phase, developed during this time span. For these reasons, Di Rosa et al. (2019c) have suggested that the late stage of the exhumation of the LU occurred during the early Miocene (~ 20-21 Ma), according to the data available for the Tenda Massif (Rossetti et al., 2015).

DISCUSSION

The tectono-metamorphic history of the units along the western edge of the Alpine Corsica

As described in the previous sections, the five continental units belonging to the LU (i.e. Volparone Breccia Slice and Castiglione-Popolasca, Piedigriggio-Prato, Croce d'Arbitro and Ghisoni units) exposed in the studied areas record a comparable deformation history but different P-T path trajectories. The multi-stepped P-T paths obtained in the Volparone Breccia Slice and for Castiglione-Popolasca, Piedigriggio-Prato and Ghisoni units using the mineral paragenesis $Chl + Ph + Ab + K\text{-}Fsp + Qz$, constrain only their exhumation trajectories up to shallower structural levels at the base of the Alpine Corsica wedge.

For Castiglione-Popolasca, Piedigriggio-Prato and Ghisoni units, the local P-T equilibrium reached during the D_{1LU} and D_{2LU} phases is given by three generations of Chl-Ph. The ranges of values at which these Chl-Ph generations reach the
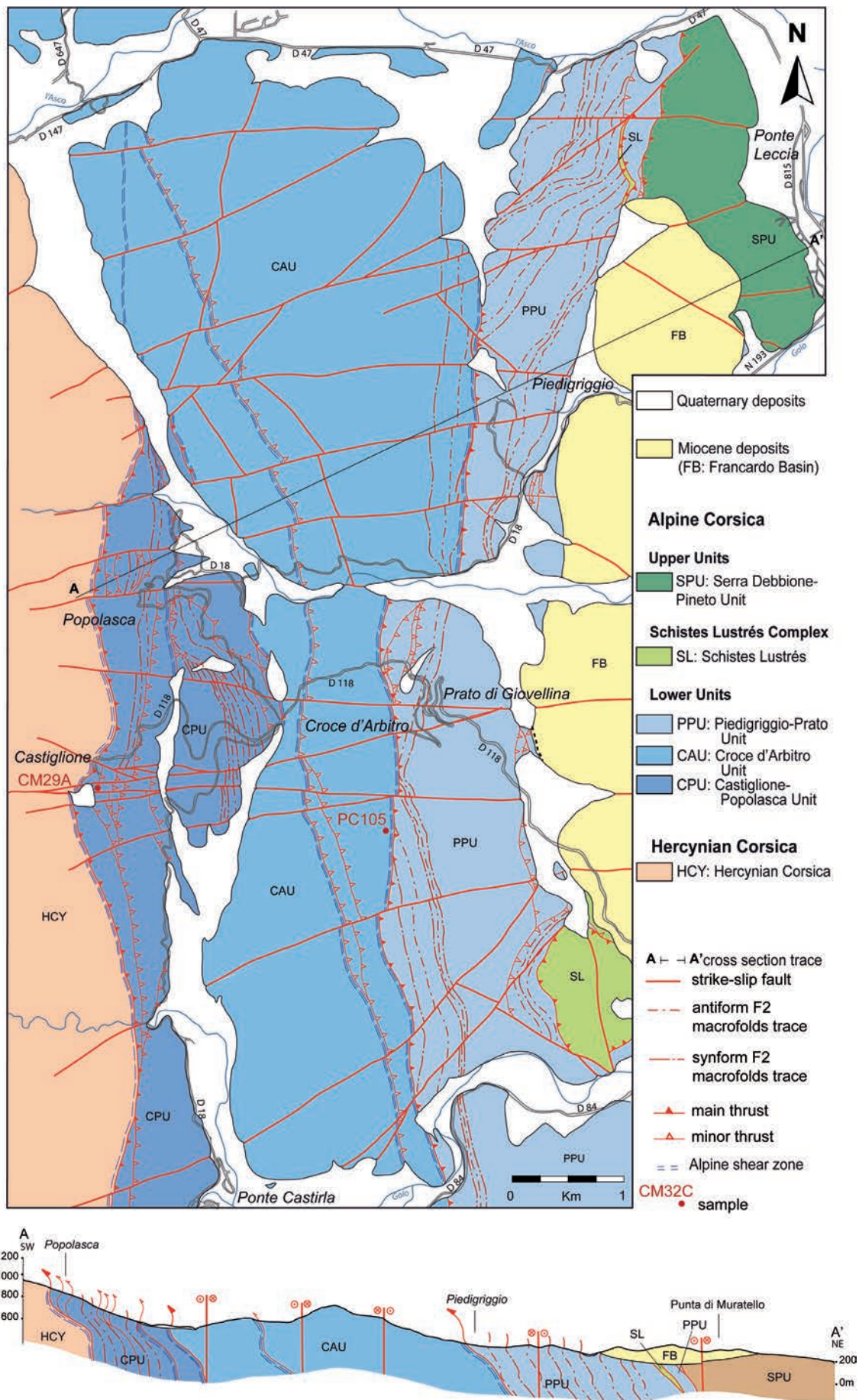
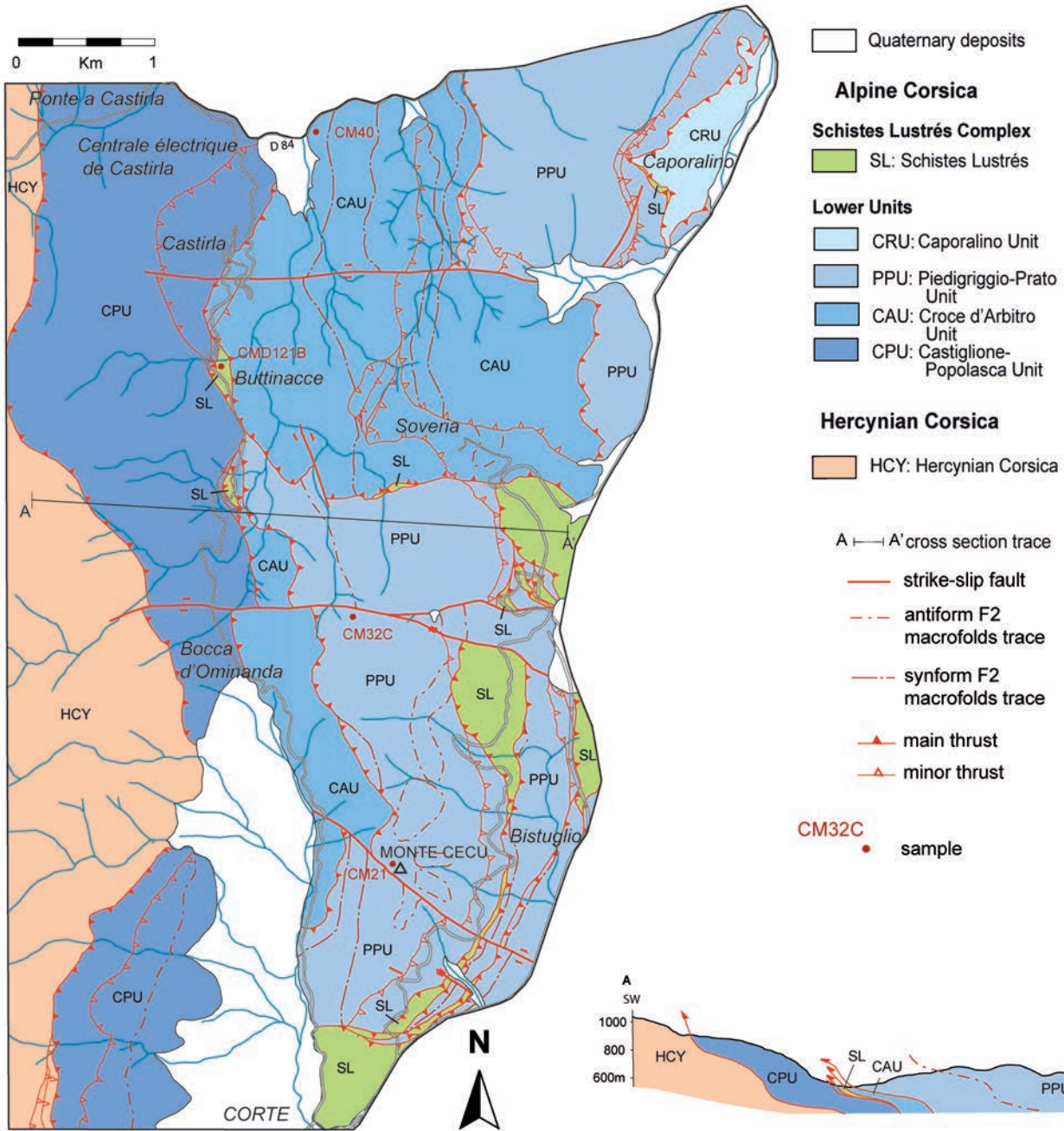Fig. 13 - Structural sketch of the Ponte Leccia/Francardo area and related cross section.

Fig. 14 - Structural sketch of the North Corte area and related cross section.

equilibrium are different for each unit, suggesting that they followed independent paths of exhumation during the D_{1LU}-D_{2LU} phases. Even if the partial re-equilibration of phyllosilicates during the polyphase deformation cannot be excluded (Lanari and Duesterhoeft, 2019), this was not observed in the studied samples.

Di Rosa et al. (2019b) discriminated isothermic and warm paths. Castiglione-Popolasca and Ghisoni units, characterized by the isothermic path, share the same structural position at the base of the LU pile, lying directly above the (cold) Hercynian Corsica. In this perspective, their isothermic paths are interpreted as an indicator of a short stay at great depth followed by a quick exhumation (Di Rosa et al., 2019b). Piedigriggio-Prato Unit, on the contrary, shows the "warm" path with an increase of T between the P-peak (early D_{1LU})

and T-peak (late D_{1LU}) of ca. 200°C. This unit occupies the uppermost position of the tectonic pile in the western Alpine Corsica, and the heating documented between the P- and T-peaks suggests that, while moving up to shallower structural levels the Piedigriggio-Prato unit experienced progressive warming, probably due to the relaxation of the geothermic field that heated up the system following the cold subduction. To register the heating, Piedigriggio-Prato Unit must have been stationed long enough at the depth estimated for the late D_{1LU}, (Di Rosa et al., 2019b). Analogous P-T paths were documented in other three continental units exposed east of Ponte Leccia, in the Pedani area (i.e. Canavaggia, Pedani and Scoltola units; Di Rosa et al., 2019b; 2019c).

Despite the differences between the isothermic and warmed paths, Castiglione-Popolasca, Piedigriggio-Prato
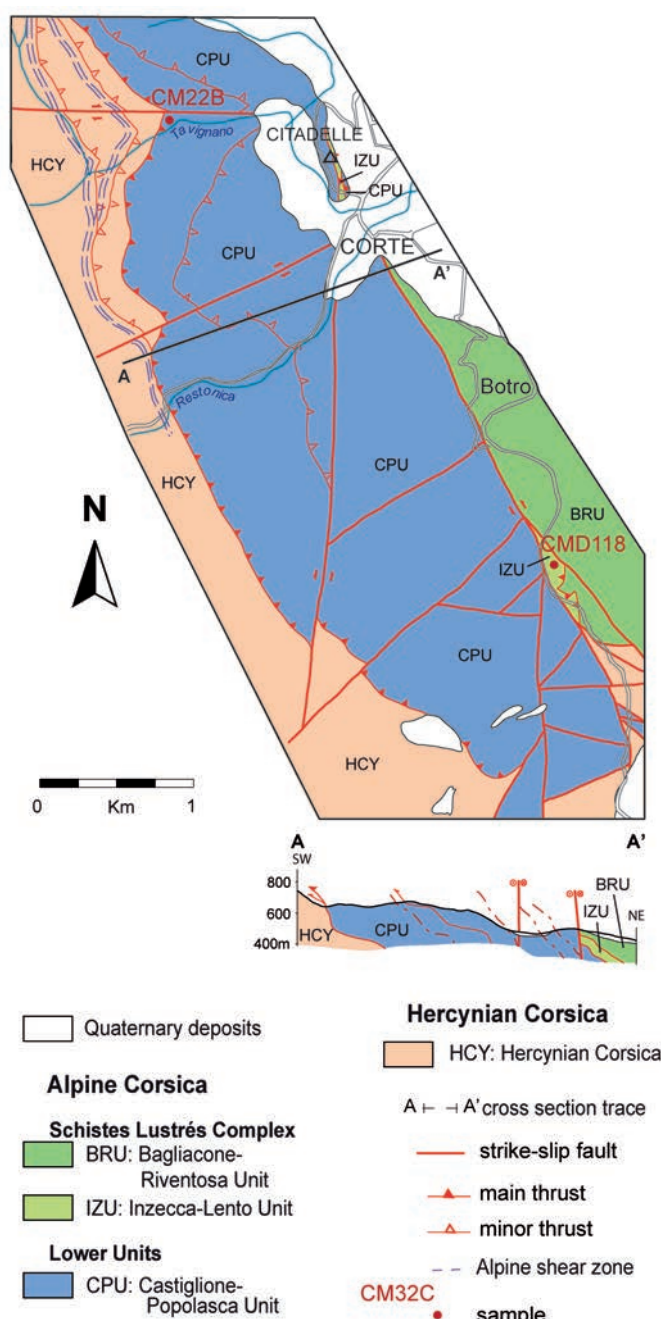
Fig. 15 - Structural sketch of the South Corte area and related cross section.

Study of the thermo-baric conditions for the Volparone Breccia Slice shows that the P- peak occurred in correspondence with the maximum temperature recorded by the unit (T-peak) at 0.60 GPa and 325°C during the D_{1LU} phase (Malasoma and Marroni, 2007). The equilibrium of Chl-Ph couples grew along the S_{2LU} foliation instead, indicate P-T conditions of 0.35 GPa and 315°C.

Even if these data are coherent with those obtained for the D_{2LU} event in the Castiglione-Popolasca, Piedigriggio-Prato and Ghisoni units, the interpretation of the P-T estimates recorded during the D_{1LU} phase of Volparone Breccia Slice deserves further discussions. In the Volparone Breccia Slice, the P-T estimates related to the D_{1LU} phase (sample BV2) overlap those obtained in sample CM29A collected in the Castiglione–Popolasca Unit (Ponte Leccia/Francardo area) for the late D_{1LU} phase (0.65-0.50 GPa, 320-345°C). Considering this correspondence and the fact that Malasoma and Marroni (2007) do not have EPMA elemental maps standardized with the spot analysis (e.g., see Di Rosa et al., 2017b; 2019b; 2020), the presence in sample BV2 (Volparone Breccia Slice) of an older generation of Chl-Ph pair (i.e. grown during the early D_{1LU}) cannot be excluded. If present, it probably crystallized during the P-peak at higher pressure (and thus compatible with a burial > 20 km) and lower temperature conditions respect to those estimated by Malasoma and Marroni (2007) for their D_{1LU} phase. Consequently, the hypothetic older generation of Chl-Ph pair could be interpreted as representative of the late D_{1LU} phase. This scenario is corroborated by mineral-chemistry investigations performed on other samples of the Volparone Breccia Slice by Malasoma and Marroni (2007), that show the presence of Si-richer phengites located on the S_{1LU} foliation implying pressure higher than ~ 0.65 GPa. The occurrence of HP-LT equilibrium in the sample BV2 implies, as in the other studied LU, the onset of the exhumation already during the D_{1LU} phase.

Unlike the other LU, the P-T conditions of Croce d'Arbitro Unit were constrained through the meta-aplitic dykes cropping out in the area of Ponte Leccia/Francardo. Thermo-baric investigations on the meta-aplitic dykes constrained the P-T conditions occurred during the D_{1LU} at 0.80-0.40 GPa and 300-370°C (Malasoma et al., 2006). Microstructures of quartz and feldspar grown along the S_{1LU} /S_{2LU} composite mylonitic foliation in the metagranitoids indicate deformation temperatures of ca. 300-400°C (Di Rosa et al., 2017a). These estimates fit well with the data obtained for the D_{1LU} phase in Castiglione-Popolasca and Piedigriggio-Prato units. Assuming "normal" strain rate and hydrolytic weakening, deformation and "metamorphic" temperature broadly coincide (Law, 2014). Consequently, since the transposition of the S_{1LU} foliation by the S_{2LU} foliation, deformation temperatures obtained from metagranitoids could be attributed to the T-peak reached during the late D_{1LU} phase.

An apparent inconsistency exists comparing the metamorphic and the deformation temperatures obtained for the Ghisoni Unit: thermobaric estimates for the late D_{1LU} indicate a temperature of 260°C, whereas microstructures of Qtz and Feld indicates deformation temperatures of 300-400°C (Di Rosa et al., 2019b). This difference is reduced considering that the quantitative method used to estimate the temperature introduces and error of ±30°C (Vidal and Parra, 2000). In addition, since the metagranitoids are affected by several systems of syn-deformational veins, the deformation temperature can be overestimated due to the higher hydrolytic weakening (Law, 2014). The T peak may be thus moved from ~ 260°C to ~ 290-300°C.

and Ghisoni Units started their exhumation during the late D_{11LU} phase (Di Rosa et al., 2017b). Assuming an average crustal geobaric gradient of 30 MPa/km (Best, 2003), the maximum depth reached by Castiglione-Popolasca and Piedigriggio-Prato units are ~ 40 and ~ 35 km, respectively, whereas for Ghisoni unit it corresponds to ~ 25 km. The P-T estimates related to the early D_{1LU} suggest a steady thermal regime of 5-6°C/km. Although this value is lower than those proposed for other continental subductions (e.g., Agard and Vitale Brovarone, 2013), it better fits with the Alpine Corsica setting, in which the European continental margin has been subducted after underthrusting of old and cold oceanic lithosphere, below an upper plate made of continental crust without arc-related magmatism (Marroni et al., 2017 and reference therein).
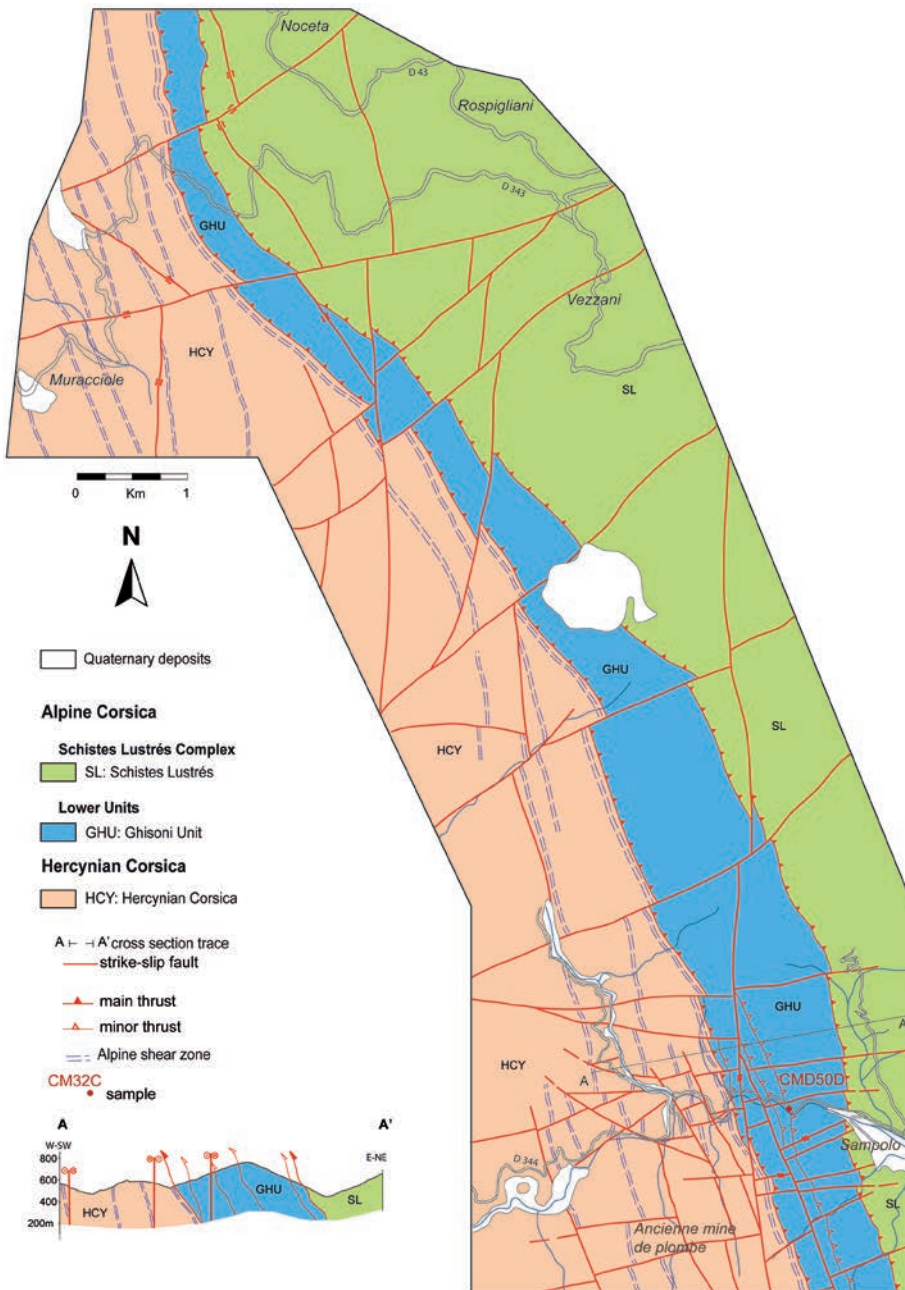
Fig. 16 - Structural sketch of the Vezzani-Ghisoni area and related cross section.

Regarding the metamorphism of the SL exposed in the western margin of Alpine Corsica, the only available data in the western side of the Alpine Corsica are those obtained from two samples of calcschists collected in the SL slices in the areas North (IZU-Buttinacce) and South (IZU-Botro) of Corte (Di Rosa et al., 2020). The two generations of Chl-Ph grown along the S_{2SL} foliation depict the retrograde path of the slices and constrain the P- and T-peaks conditions (Tab. 3). The P and T differences obtained for the two samples suggest that these slices followed different exhumation paths. Considering a subduction gradient of 6-11°C/km, the maximum depth reached by the SL Corte slices is ~ 12 km, compatible with those estimated for the SL in the Western Alps (Agard et al., 2001; Plunder et al., 2012).

Additional information on the P-T peak conditions reached by the SL have been estimated by Levi et al. (2007) in the Lento Unit, exposed east of Ponte Leccia. The P-peak estimates obtained by Levi et al. (2007) (P = 0.93-0.70 GPa)

partly overlap those of the SL Corte slices (IZU-Buttinacce: 0.85-0.70 GPa; IZU-Botro: 1.00-0.85 GPa) of Corte obtained by Di Rosa et al. (2020). The excess in temperatures of more than 100°C in the Lento Unit respect to the SL Corte slices (240-275°C: IZU-Buttinacce and 200-250°C: IZU-Botro; by Di Rosa et al., 2020) can be explained by considering the different structural position: while the SL Corte slices are close to the "cold" Hercynian Corsica, the Lento Unit is located far to the east at upper structural levels.

As a whole, P-T data related to LU and SL suggest that the units followed different exhumation trajectories until their coupling, which likely occurred at the end of the D_{2LU}/D_{3SL} (Di Rosa et al., 2020). This timing is constrained by the folding of the entire nappe pile that occurred during the D_{3LU}/D_{4SL} phase. A similar scenario has been described by Di Rosa et al., 2019c) in the Cima Pedani area, where the Lento Unit (SL) is staked above three continental units (LU) and the entire pile is subsequently folded during the D_{3LU}/D_{4SL} ductile event.

Similarly, the coupling between the LU and UU occurred during the late stage of the D_{2LU}. As clearly observed in the North Balagne area by Malasoma and Marroni (2007), the coupling is achieved through N-S trending top-to-the W shear zones that produced the delamination and the thinning of the LU into slices whose thickness does not exceed a few tens of meters (Rossi et al., 2001; Marroni and Pandolfi, 2003; Pandolfi et al., 2016). The depth of the coupling cannot be determined, but it is achieved at very shallow structural levels, as suggested by the features of the D_{2UU} phase.

The thermo-baric and structural data collected in the LU, UU and SL indicate that the LU were exhumed at the base of an orogenic wedge represented by the previously accreted stack of SL and UU at its top. The LU started the exhumation path during the $D_{1LU,}$ and only at the end of the D_{2LU} (i.e. at depth of 10-15 km) they were coupled with the SL and UU. Subsequently, the entire stack (LU, SL and UU) was deformed and exhumed as a single body during the $D_{3LU}/D_{4SL}/D_{3UU}$ phase up to a complete exposure at the surface in the Burdigalian (i.e. the age of the oldest deposits of the Francardo Basin).

The relationships between the oceanic and continental units as witnesses of a "migrating" plate interface

In the sections above, we described the western boundary of the Alpine Corsica as the location where the oceanic and continental units coupled at different structural levels during their exhumation paths along the plate interface, i.e. at the base of the orogenic wedge. In the studied areas, the coupling occurred before the last ductile event ($D_{3LU}/D_{4SL}/D_{3UU}$ phases) that deformed the tectonic contacts between the different units.

Regardless the depth at which the coupling occurs, it is worthy to note that the tectonic coupling involves rock volumes that experienced independent burial/exhumation processes at different times and P-T conditions. Since the west-dipping subduction first involved the oceanic crust of the Ligure-Piemontese oceanic basin, and then the thinned European continental margin, a progressively younger set of ages of deformation and metamorphism moving from the oceanic, ocean/continent transition to continental-affinity units would be expected (e.g., Strzerzynski et al., 2012).

The SL, representing the oceanic crust involved in the subduction since Late Cretaceous, were deformed and metamorphosed under blueschist/eclogite facies conditions during their transfer to the Alpine accretionary wedge, and to the Alpine Corsica orogenic wedge (i.e. D_{1SL}-D_{3SL} phases). The SL stationed at the base of the orogenic wedge until their coupling with the LU and final exhumation up to the surface.

The UU were derived by the Ligure-Piemontese oceanic lithosphere but they experienced involvement in the subduction at shallow structural level, probably during the Paleocene (Marroni and Pandolfi, 2003; Pandolfi et al., 2016). In this framework, the UU experienced underplating at a depth of 10-12 km (D_{1UU} phase) followed by a progressive exhumation (D_{2UU} and D_{3UU} phases). During exhumation, coupling with the LU occurred at the end of the D_{2UU} phase and before the D_{3UU} phase.

The LU were involved in the continental subduction since the late Eocene, as suggested by the presence of Tertiary deposits coherently deformed and metamorphosed during subduction (Di Rosa et al., 2020 and reference therein). The LU registered the peak metamorphism under blueschist facies conditions (i.e. early D_{1LU} phase) and then were gradually exhumed following different P-T paths and at different rates during the D_{2LU} phase.

Recent studies provided a record of the tectono-metamorphic evolution of continental and oceanic units in order to understand the mechanisms of slicing of oceanic units at the base of the orogenic wedge after their accretion, and their coupling with the continental units during their rising up along the plate interface (Agard et al., 2009; Agard and Vitale Brovarone, 2013; Angiboust et al., 2012; Brun and Faccenna, 2008; Di Rosa et al., 2019c; Lapen et al., 2007; Plunder et al., 2012; 2015). We have shown here that the western edge of the Alpine Corsica shows a more complex scenario, where slices of SL are found not only at the top of the LU, but also interposed between them as observed North and South of Corte (Figs. 14 and 15). The juxtaposition of LU with SL and UU, developed along the plate interface after the accretion of the LU to the orogenic wedge represented by the SL and UU stack (Di Rosa et al, 2017b; 2019c; Malasoma and Marroni, 2007; Molli et al., 2006). Moreover, the SL slices between the LU testify that the LU during their exhumation were able to rip off slices of the orogenic wedge (i.e. SL) and to tectonically incorporate them (Di Rosa et al., 2020). This mechanism can be described as a basal tectonic erosion similar which was suggested to explain the dragging and translation of pieces of orogenic wedge (von Huene and Scholl, 1991; Clift and Vannucchi, 2004; Sallarés and Ranero, 2005; Agard et al., 2018). Di Rosa et al. (2020) proposed such a model through which the re-activation of weak rheological horizon within the orogenic wedge as shear zones would allow the mass dragging along the base of the wedge and their rising up between the plate interface and the wedge base. The (re)moving of thin slices of oceanic material (in this case the SL) was probably facilitated by the buoyancy-driven exhumation of large volume of continental units (here represented by the LU) up to the surface (Di Rosa et al., 2020) as proposed for other continental subduction settings (Angiboust et al., 2009; Plunder et al., 2012; 2015).

The geodynamic setting of the Lower Units - Schistes Lustrés Complex- Upper Units coupling

In Alpine Corsica, the subduction-related tectono-metamorphic phases have been documented in the LU, SL and UU. All these tectono-metamorphic phases are achieved during a geodynamic history that started in the Late Cretaceous by an east-dipping subduction of the oceanic crust of the Ligure-Piemontese oceanic basin (i.e. the SL and UU) below the Adria continental margin, as depicted in most geodynamic reconstructions (Mattauer and Proust, 1976; Warburton, 1986; Schmid et al., 1996; Malavieille et al., 1998; Molli et al., 2006; Handy et al., 2010; Malusà et al., 2015; Marroni et al., 2017; Di Rosa et al., 2020). Convergence resulted in the progressive involvement of the thinned European continental margin (i.e. the LU) in the subduction zone and then in the collision between the European continental margin and the Alpine wedge-Adria microplate system.

According to this geodynamic model, the SL registered a HP-LT metamorphic imprint ranging in age from Late Cretaceous (Lahondère and Guerrot, 1997; Maluski, 1977; Brunet et al., 2000) to late Eocene (Brunet et al., 2000; Martin et al., 2011; Vitale Brovarone and Herwartz, 2013). Regarding the LU, the data on the HP-LT metamorphism are available only for the Tenda Massif where the ages span from early to late Eocene (Brunet et al., 2000; Maggi et al., 2012). Similar ages were also obtained for the most external Alpine shear zones affecting the Variscan basement (Di Vincenzo et al., 2016).

No data are available for the LU located along the western edge of the Alpine Corsica. However, the occurrence of *Nummulites* sp. (middle to late Eocene, Bezert and Caby, 1988) in the youngest lithotypes of the LU (i.e. Metabreccia and Metasandstone Fms.) indicate that their subduction started at least in the late Eocene (Di Rosa et al., 2020 and reference therein). In the UU, the deformation history is constrained only by the age of the youngest deposits involved in the deformation (i.e. Late Cretaceous age of the Narbinco Flysch; Marino et al., 1995).

After their involvement into the subduction zone, the SL, LU and UU underwent exhumation up to their exposure at the surface in the early Miocene, when the older deposits of the Francardo Basin unconformably seal the structure of the SL and LU in the Ponte Leccia - Francardo area (Ferrandini et al., 2003; Alessandri et al., 1977; Malasoma et al., 2020).

Concerning the LU, the available data indicate a progressive involvement of the continental crust from early Eocene for the Tenda Massif and from late Eocene for the metamorphic continental units located at the western edge of Alpine Corsica (Egal, 1992; Malavieille et al., 1998; Molli et al., 2006; Malasoma et al., 2006; Di Rosa et al., 2017a: 2017b; 2019b; 2019c). Burial and exhumation of the continental crust units was followed by exposure at the surface in the early Miocene.

In the time span between late Eocene and early Miocene, the LU located along the western edge of the Alpine Corsica registered a HP-LT event (early D_{1LU} phase) achieved during their burial at deep structural level (~ 40 km for Castiglione-Popolasca Unit, ~ 35 km for Piedigriggio-Prato Unit, ~ 25 km for Ghisoni Unit and ~ 20 km for Volparone Breccia Slice). The path followed by each unit started from the late D_{1LU} phase up to the end of the D_{2LU} phase, when all the units reached a depth of ~ 10 km and were coupled with the SL and the UU. The final stage of the exhumation ($D_{3LU}/D_{4SL}/D_{3UU}$ phases) affected the newly formed tectonic stack as result of vertical shortening.

From late Eocene to early Miocene, the southeastward retreat of the W-dipping slab produced a regional shift from syn-orogenic to post-orogenic stage (e.g., Doglioni, 1991; Gueguen et al., 1998; Jolivet et al., 1998, 2015; Speranza et al., 2002; Faccenna et al., 2004). The shift most probably occurred in the uppermost early Oligocene, at the transition to the late Oligocene (Faccenna et al., 2002; Jolivet et al., 2015; Beaudoin et al., 2017).

Since the absolute ages of the D_{1LU} and D_{2LU} are lacking, the LU exhumation-related deformations can be ascribed either to the syn-orogenic stage or to the post-orogenic one. As described in several papers (Daniel et al., 1996; Gueydan et al., 2003; Maggi et al., 2012; Di Rosa et al., 2019b), the late D_{1LU} and D_{2LU} probably occurred during the syn-orogenic exhumation. Coherent with these reconstructions, Di Rosa et al. (2020) have proposed a correlation between the D_2 phase in the Tenda Massif dated by Rossetti et al. (2015) at ~27-32 Ma with the last stage of D_{2LU} phase, during which the coupling between the LU, SL and UU occurred.

The last ductile event (i.e. the D_{3LU}) can be thus related to the post-orogenic collapse of the wedge. This was due, in turn, to the extensional regime responsible of the opening of the Ligurian-Provençal back-arc basin that progressively affect the whole Corsica Island (Chamot-Rooke et al., 1999; Faccenna et al., 2008). Such interpretation is supported by the fission track ages available for the western edge of the Alpine Corsica that show a rejuvenation trend from west to east along the Alpine Corsica (Danišik et al., 2007).

Finally, it is possible to assume a scenario where the exhumation history of the LU occurred at different geodynamic setting. Following this reconstruction, the late D_{1LU} and D_{2LU} occurred during the syn-orogenic exhumation (late Eocene-early Oligocene) whereas the D_{3LU} can be associated with the extensional event related to the post-orogenic collapse. As a consequence, the coupling between LU, SL and UU occurred at the transition between these two different geodynamic regimes.

CONCLUSIONS

The review of the geological background (i.e. the stratigraphic features, deformation history, metamorphic P-T path and tectonic setting) performed for the five selected areas of Corsica Island has provided new insights on the relationships between the continental and oceanic units cropping out along the western edge of the Alpine Corsica (Fig. 17). The investigated areas are, from the north to the south: North Balagne, Ponte Leccia-Francardo, North of Corte, South of Corte and Vezzani-Ghisoni.

The collected data indicate that:

1) the continental units (i.e. LU) represent fragments of the thinned European continental margin whereas the oceanic units (i.e. SL and UU) represent remnants of the Ligure-Piemontese oceanic basin and its transition to the continental domain;

2) the SL and UU are found not only at the top of the LU, as stated in the majority of the available literature, but also as imbricated slices within the LU (Fig. 17). In particular, slices of UU are associated with LU in the North Balagne area and with SL in the Ponte Leccia-Francardo and North of Corte areas. In the South of Corte and Vezzani-Ghisoni areas, the SL occurs only at the top of the LU;

3) the LU registered a polyphase tectono-metamorphic history from D_{1LU} to D_{3LU} phase. They were buried at 20-40 km of depth (HP-LT event; early D_{1LU} phase) and then exhumed following different trajectories during the late D_{1LU} phase up to the end of the D_{2LU} phase. After the D_{2LU} phase, the exhumation of the LU is accommodated by the D_{3LU} up to their exposure at the surface;

4) the LU, SL and UU are coupled at about 10-15 km of depth through N-S striking, top-to-the W shear zones developed during the late stage of the $D_{2LU}/D_{3SL}/D_{2UU}$ phases. The top-to-the W shear zones are in turn deformed during the last event of exhumation ($D_{3LU}/D_{4SL}/D_{3UU}$ phases);

5) before their coupling, the SL, UU and LU recorded independent tectono-metamorphic histories achieved at different times during the convergence-related processes responsible for the closure of the Ligure-Piemontese oceanic basin. This closure started in the Late Cretaceous by an E-dipping subduction of the oceanic crust of the Ligure-Piemontese oceanic basin. The subduction continued until late Paleocene with the progressive involvement of the thinned European continental margin. After their involvement in the subduction zone, the SL, LU and UU underwent to a progressive exhumation up to their exposure at the surface in the early Miocene (i.e. the age of the deposits of the Francardo Basin that unconformably seal the structure of the SL and LU in the Ponte Leccia - Francardo area);

6) the LU exhumation occurred during the shift of geodynamic regime of the Alpine-Apennine system. In this hypothesis, the late D_{1LU} and D_{2LU} occurred during the
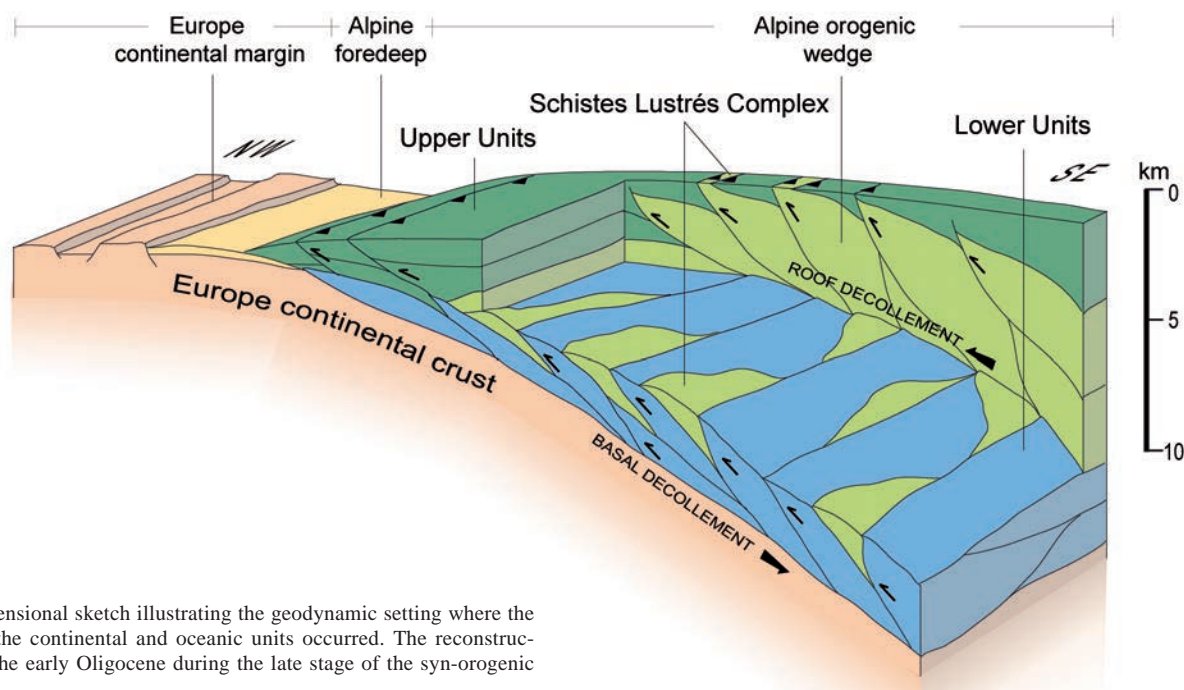
Fig.17 - Three dimensional sketch illustrating the geodynamic setting where the coupling between the continental and oceanic units occurred. The reconstruction is referred to the early Oligocene during the late stage of the syn-orogenic exhumation.

syn-orogenic exhumation (late Eocene-early Oligocene), whereas the D_{3LU} can be associated with the extensional tectonics started in the late Oligocene, as the result of the post-orogenic collapse. Thus, the coupling between the LU, SL and UU occurred at the switch between these two different geodynamic regimes. This hypothesis, proposed for the LU exposed in the western edge of the Alpine Corsica, does not exclude the possibility that the coupling between continental and oceanic rocks may occurred earlier, at different depths and different times;

7) the data presented in this paper documented the complexity of the tectono-metamorphic processes occurring in a convergent margin during the transition from oceanic subduction to continental collision. The full picture of such tectono-metamorphic events can be only achieved using a multidisciplinary approach performed from map- to micro-scale.

REFERENCES

Abbate E., Bortolotti V. and Principi G., 1980. Appennine ophiolites: a peculiar oceanic crust. Ofioliti, Spec. Iss., 1: 59-96.

Agard P. and Vitale Brovarone A., 2013. Thermal regime of continental subduction: the record from exhumed HP-LT terranes (New Caledonia, Oman, Corsica). Tectonophysics, 601: 206-215.

Agard P., Jolivet L. and Goffé B., 2001. Tectonometamorphic evolution of the Schistes Lustrés complex: implications for the exhumation of HP and UHP rocks in the Western Alps. Bull. Soc. Géol. France, 175 (5): 617-636.

Agard P., Omrani J., Jolivet L., Whitechurch H., Vrielynk B. Spakman W., Monié P., Meyer B. and Wortel R., 2011. Zagros orogeny: a subduction dominated processes. Geol. Mag., 148 (5-6): 692-725.

Agard P., Plunder A., Angiboust S., Bonnet G. and Ruh J., 2018. The subduction plate interference: rock record and mechanical coupling (from long to short timescales). Lithos, 320-321: 537-566.

Agard P., Yamato P., Jolivet L. and Burov E., 2009. Exhumation of oceanic blueschists and eclogites in the subduction channel: timing and mechanisms. Earth Sci. Rev., 92: 53-79.

Alessandri J.A., Magné J., Pilot M.D. and Samuel E., 1977. Le Miocène de la région de Corte-Francardo. Bull. Soc. Sci. Hist. Nat. Corse, 622 : 51-54.

Amaudric du Chaffaut S., 1975. L'unité de Corte: un témoin de "Piémontais externe" en Corse? Bull. Soc. Géol. France, 7: 739-745.

Amaudric du Chaffaut S. and Saliot P., 1979. La region de Corte: secteur-clé pour la comprehension du métamorphisme alpin en Corse. Bull. Soc. Géol. France, 21: 149-154.

Amaudric du Chaffaut S., Bonin B., Caron J.M., Conchon O. and Rossi P., 1985. Carte Géologique de la France (1/50000), feuille Venaco (1114). B.R.G.M, Orleans, France.

Amaudric du Chaffaut S., Caron J.M., Delcey R. and Lemoine M., 1972. Données nouvelles sur la stratigraphie des schistes lustrés de Corse: La série de l'Inzecca. Comparaison avec les Alpes Occidentales et l'Apennin ligure. Acad. Sci. Paris, 275: 2611-2614.

Amaudric du Chaffaut S., Kienast J.R. and Saliot P., 1976. Répartition de quelques minéraux de métamorphisme alpin en Corse. Bull. Soc. Géol. France, 18 (5): 1179-1182.

Angiboust S., Agard P., Jolivet L. and Beyssac O., 2009. The Zermatt-Saas ophiolite: the largest (60-km wide) and deepest (c. 70-80 km) continuous slice of oceanic lithosphere detached from a subduction zone? Terra Nova, 21: 171-180.

Angiboust S., Wolf S., Burov E., Agard P. and Yamato P., 2012. Effect of fluid circulation on subduction interface tectonic processes: insights from thermo-mechanical numerical modelling. Earth Planet. Sci. Lett., 357-358: 238-248.

Argand E., 1924. Des Alpes et de l'Afrique. Bull. Soc. Vaudoise Sci. Nat., 55: 233-236.

Beaudoin A., Augier R., Jolivet L., Jourdon A., Raimbourg H., Scaillet S. and Cardello G.L., 2017. Deformation behavior of continental crust during subduction an exhumation: strain distribution over the Tenda Massif (Alpine Corsica, France). Tectonophysics, 705: 12-32.

Beltrando M., Zibra I., Montanini A. and Tribuzio R., 2013. Crustal thinning and exhumation along a fossil magma-poor distal margin preserved in Corsica: A hot rift to drift transition? Lithos, 169-189: 99-112.

Berman R.G., 1991. Thermobarometry using multiequilibrium calculations: a new technique with petrologic applications. Can. Miner., 29: 833-855.

Berno D., Sanfilippo A., Zanetti A. and Tribuzio R., 2019. Reactive melt migration controls the trace element budget of the lower oceanic crust: insights from the troctolite-olivine gabbro association of the Pineto Ophiolite (Corsica, France). Ofioliti, 44 (2): 71-82.

Best M.G., 2003. Igneous and metamorphic petrology. Brigham Young Univ., Blackwell Publ., 2nd ed., 758 pp.

Bezert P. and Caby R., 1988. Sur l'âge post-bartonien des événements tectonométamorphiques alpins en bordure orientale de la Corse cristalline (Nord de Corte). Boll. Soc. Géol. France, 4 (6): 965-971.

Bill M., Bussy F., Cosca M.A., Masson H. and Hunziker J.C., 1997. High-precision Upb and ^{40}Ar/^{39}Ar dating of an Alpine ophiolite (Gets nappe, French Alps): Ecl. Geol. Helv., 90: 43-54.

Boccaletti M., Elter P. and Guazzone G., 1971. Plate tectonic models for the development of the Western Alps and Northern Apennines. Nature, 234: 108-111.

Bracciali L., Marroni M., Pandolfi L. and Rocchi S., 2007. Petrography and geochemistry of western Tethys Mesozoic sedimentary covers (Alpine Corsica and Northern Apennines): a valuable tool in constraining sediment provenance and margin configuration. In: J. Arribas, S. Critelli, M.J. Johnsson (Eds.), Sedimentary provenance and petrogenesis: perspectives from petrography and geochemistry. Geol. Soc. Am. Spec. Pap., 420: 73-93.

Brun J.P. and Faccenna C., 2008. Exhumation of high-pressure rocks driven by slab rollback. Earth Planet. Sci. Lett., 272 (1): 1-7.

Brunet C., Monié P., Jolivet L. and Cadet J.P., 2000. Migration of compression and extension in the Tyrrhenian Sea, insights from ^{40}Ar/^{39}Ar ages on micas along a transect from Corsica to Tuscany. Tectonophysics, 321: 127-155.

Burkhard M., 1992. Calcite twins, their geometry, appearance and significance as stress-strain markers and indicators of tectonic regime: a review. J. Struct. Geol., 20: 1-18.

Cabanis B., Cochemé J.J., Vellutini P.J., Joron J.L. and Treuil M., 1990. Post-collisional Permian volcanism in northwestern Corsica: an assessment based on mineralogy and trace-element geochemistry. J. Volc. Geotherm. Res., 44: 51-67.

Caron J.M., 1994. Metamorphism and deformation in Alpine Corsica. Schweiz. Miner. Petr. Mitt., 74 (1): 105-114.

Caron J.M. and Delcey R., 1979. Lithostratigraphie des Schistes Lustrés corses: diversité des séries post-ophiolitiques. C.R. Acad. Sci. Paris, 288: 1525-1528.

Caron J.M., Kienast J.R. and Triboulet C., 1981. High-pressure/low-temperature metamorphism and polyphase Alpine deformation at Sant'Andrea di Cotone (Eastern Corsica, France). Tectonophysics, 78: 419-451.

Cathelineau M., 1988. Cation site occupancy in chlorites and illites as a function of temperature. Clay Miner., 23: 471-485.

Cathelineau M. and Nieva D., 1985. A chlorite solid solution geothermometer. The Los Azufres (Mexico) geothermal system. Contrib. Miner. Petr., 91: 235-224.

Cavazza W., DeCelles P.G., Fellin M.G. and Paganelli L., 2007. The Miocene Saint-Florent Basin in northern Corsica: stratigraphy, sedimentology, and tectonic implications. Basin Res., 19 (4): 507-527.

Cavazza W., Gandolfi G. and Paganelli L., 2018. Reconstructing the Alpine orogenic wedge and its foreland basin: The petrologic transition from Cretaceous passive-margin to Eocene foreland sedimentation in northern Corsica (France). In: R.V. Ingersoll, T.F. Lawton and S.A. Graham (Eds.), Tectonics, sedimentary basins, and provenance: A celebration of the career of William R. Dickinson. Geol. Soc. Am. Spec. Pap., 540, doi:https://doi.org/10.1130/2018.2540(31)

Cavazza W., Zattin M., Ventura B. and Zuffa G.G., 2001. Apatite fission track analysis of Neogene exhumation in northern Corsica (France). Terra Nova, 13: 51-57.

Ceriani S., Fügenschuh B. and Schmid S.M., 2001. Multi-stage thrusting at the "Penninic Front" in the Western Alps between Mont Blanc and Pelvoux massifs. Int. J. Earth Sci. (Geol. Rundsch), 90: 685-702.

Chamot-Rooke N., Gaulier J.M and Jestin F., 1999. Constraints on Moho depth and crustal thickness in the Liguro-Provençal basin from a 3D gravity inversion: geodynamic implications. In: B. Durand, L. Jolivet, F. Horvath and M. Sérranne (Eds.), The Mediterranean basin: Tertiary extenson within the Alpine Orogen. Geol. Soc. London Spec. Publ., 156: 37-61.

Chemenda A.I., Mattauer M., Malavieille J. and Bokun A.N., 1995. A mechanism for syn-collisional deep rock exhumation and associated normal faulting: Results from physical modeling. Earth Planet. Sci. Lett., 132: 225-232.

Chopin C., Beyssac O., Bernard S. and Malavieille J., 2008. Aragonite-grossular intergrowths in eclogite-facies marble, Alpine Corsica. Eur. J. Miner., 20: 857-865.

Clift P. and Vannucchi P., 2004. Controls on tectonic accretion versus erosion in subduction zones: implications for the origin and recycling of the continental crust. Rev. Geophys., 42: RG2001.

Dallan L. and Nardi R., 1984. Ipotesi dell'evoluzione dei domini "liguri" della Corsica nel quadro della paleogeografia e della paleotettonica delle unità alpine. Boll. Soc. Geol. It., 103: 515-527.

Dallan L. and Puccinelli A., 1995. Geologia della regione tra Bastia e St-Florent (Corsica Settentrionale). Boll. Soc. Geol. It., 114: 23-66.

Daniel J.M., Jolivet L., Goffé B. and Poinssot C., 1996. Crustal-scale strain partitioning: footwall deformation below the Alpine Oligo-Miocene detachment of Corsica. J. Struct. Geol., 18 (1): 41-59.

Danisik M., Kuhlemann J., Dunkl I., Székely B. and Frisch W., 2007. Burial and exhumation of Corsica (France) in the light of fission track data. Tectonics, 26: TC1001.

Deseta N., Andersen T.B. and Ashwal L.D., 2014. A weakening mechanism for intermediate-depht seismicity? Detailed petrographic and microtextural observations from bleschist facies pseudotachylites, Cape Corse, Corsica. Tectonophysics, 610: 138-149.

De Wever P., Danielan T., Durand-Delga M., Cordey F. and Kito F., 1987. Datations des radiolarites post-ophiolitique de Corse alpine à l'aide des radiolaires. C.R. Acad. Sci., Paris, 305: 893-900.

Di Rosa M., De Giorgi A., Marroni M. and Pandolfi L., 2017a. Geology of the area between Golo and Tavignano Valleys (Central Corsica): a snapshot of the continental metamorphic units of Alpine Corsica. J. Maps, 13: 644-653.

Di Rosa M., De Giorgi A., Marroni M. and Vidal O., 2017b. Syn-convergence exhumation of continental crust: evidence from structural and metamorphic analysis of the Monte Cecu area, Alpine Corsica (Northern Corsica, France). Geol. J., 52: 919-937.

Di Rosa M., Frassi C., Marroni M., Meneghini F. and Pandolfi L. 2019a. Did the "Autochthonous" European foreland of Corsica Island (France) experience Alpine subduction? Terra Nova, 32: 34-43.

Di Rosa M., Frassi C., Meneghini F., Marroni M., Pandolfi L. and De Giorgi A., 2019b. Tectono-metamorphic evolution in the European continental margin involved in the Alpine subduction: new insights from the Alpine Corsica, France. C.R. Acad. Sci. Paris, 351 (5): 384-394.

Di Rosa M., Meneghini F., Marroni M., Frassi C. and Pandolfi L., 2020. The coupling of high-pressure oceanic and continental units in Alpine Corsica: evidence for syn-exhumation tectonic erosion at the roof of the plate interface. Lithos, 354-355: 105328, https://doi.org/10.1016/j.lithos.2019.105328.

Di Rosa M., Meneghini F., Marroni M., Hobbs N. and Vidal O., 2019c. The exhumation of continental crust in collisional belts: insights from the deep structure of Alpine Corsica in the Cima Pedani area. J. Geol., 127 (3): 263-288.

Di Vincenzo G., Grande A., Prosser G., Cavazza W. and DeCelles P.G., 2016. ^{40}Ar/^{39}Ar laser dating of ductile shear zones from central Corsica (France): Evidence of Alpine (middle to late Eocene) syn-burial shearing in Variscan granitoids. Lithos, 262: 369-383.

Doglioni C., 1991. A proposal of kinematic modelling for W-dipping subductions - Possible applications to the Tyrrhenian-Apennines system. Terra Nova, 3: 423-434.

Doglioni C., Mongelli F. and Pialli G., 1998. Boudinage of the Alpine belt in the Apenninic back-arc. Mem. Soc. Geol. It., 52: 457-468.

Donatio D., Marroni M. and Rocchi S., 2013. Serpentinization history in mantle secrion from a fossil slow-spreading ridge sequence: Evidences from Pomaia quarry (Southern Tuscany, Italy). Ofioliti, 38 (1): 15-28.

Dubacq B., Vidal O. and De Andrade V., 2010. Dehydration of dioctahedral aluminous phyllosilicates: thermodynamic modelling and implications for thermobarometric estimates. Contrib. Miner. Petr., 159: 159-174.

Durand-Delga M., 1974. La Corse. Géol. France, 2: 465-478.

Durand-Delga M., 1984. Principaux traits de la Corse Alpine et correlations avec les Alpes Ligures. Mem. Soc. Geol. It., 28: 285-329.

Durand-Delga M., Fondecave-Wallez M.J. and Rossi P., 2005. L'unité ophiolitique de Pineto (Corse): signification du détritisme continental dans sa couverture de flysch albo-cénomanien. C.. Geosci., 337 (12): 1084-1095.

Durand-Delga M., Peybernès B. and Rossi P., 1997. Arguments en faveur de la position, au Jurassique, des ophiolites de Balagne (Haute-Corse, France) au voisinage de la marge continentale européenne. C.R. Acad. Sci. Paris, 325: 973-981.

Egal E., 1992. Structures and tectonic evolution of the external zone of Alpine Corsica. J. Struct. Geol., 14: 1215-1228.

Egal E. and Caron J.M., 1988. Tectonique polyphasée dans l'Eocène autochtone à la bordure ouest de la Nappe de Balagne (Corse). Bull. Soc. Géol. France, 8: 315-321.

Elter P. and Pertusati. P.C., 1973. Considerazioni sul limite Alpi-Appennino e sulle relazioni con l'arco della Alpi Occidentali. Mem. Soc. Geol. It., 12: 359-375.

Faccenna C., Speranza F., Caracciolo F.D.A., Mattei M. and Oggiano G., 2002. Extensional tectonics on Sardinia (Italy)): insights into the arc-back-arc transitional regime. Tectonophysics, 356 (4): 213-232.

Faccenna C., Piromallo C., Crespo-Blanc L., Jolivet L. and Rossetti F., 2004. Lateral slab deformation and the origin of Western Mediterranean arcs. Tectonics, 23: TC1012.

Faccenna C., Becker T.W., Auer L., Billi A., Boschi L., Brun J.P., Capitanio F.A., Funiciello F., Horvàth F., Jolivet L., Piromallo C., Royden L., Rossetti F. and Serpellini E., 2008. Mantle dynamics in the Mediterranean. Rev. Geophys., 52: 283-332, doi:10.1002/2013RG000444.

Faure M. and Malavieille J., 1981. Étude structurale d'un cisaillement ductile: le charriage ophiolitique corse dans la région de Bastia. Bull. Soc. Géol. France, 23 (4): 335-343.

Favre P. and Stampfli G.M., 1992. From rifting to passive margin: the example of the Red Sea, Central Atlantic and Alpine Tethys. Tectonophysics, 215: 69-97.

Fellin M.G., Picotti V. and Zattin M., 2005. Neogene to Quaternary rifting and inversion in Corsica: Retreat and collision in the western Mediterranean. Tectonics, 24 (1): doi:10.1029/2003TC001613.

Ferrandini M., Ferrandini J., Loye-Pilot M.D., Butterlin J., Cravatte J. and Janin M.C., 1998. Le Miocène du bassin de Saint-Florent (Corse): modalités de la transgression du Burdigalien supérieur et mise en évidence du Serravallien. Geobios, 31 (1): 125-137.

Ferrandini J., Ferrandini M., Rossi P. and Savary-Sismondini B., 2010. Définition et datation de la formation de Venaco (Corse): dépôt d'origine gravitaire d'âge Priabonien. C.R. Geosci., 342: 921-929.

Ferrandini J., Gattacceca J., Ferrandini M., Deino A. and Janin M.C., 2003. Chronostratigraphie et paléomagnétisme des dépôts oligo-miocènes de Corse: implications géodynamiques pour l'ouverture du bassin liguro-provençal. Bull. Soc. Géol. France, 174 (4): 357-371.

Fournier M., Jolivet L., Goffé B. and Dubois R., 1991. The Alpine Corsica metamorphic core complex. Tectonics, 10: 1173-1186.

Froitzheim N. and Manatschal G., 1996. Kinematics of Jurassic rifting, mantle exhumation, passive margin formation in the Austroalpine and Penninic nappes (Eastern Switzerland). Geol. Soc. Am. Bull., 108: 1120-1333.

Garfagnoli F., Menna F., Pandeli E. and Principi G., 2009. Alpine metamorphic and tectonic evolution of the Inzecca-Ghisoni area (southern Alpine Corsica, France). Geol. J., 44: 191-210.

Gattacceca J., Deino A., Rizzo R., Jones D.S., Henry B., Beaudoin B. and Vedeboin F., 2007. Miocene rotation of Sardinia: new paleomagnetic and geochronological constraints and geodynamic implications. Earth Planet. Sci. Lett., 258: 359-377.

Gibbons W. and Horak J., 1984. Alpine metamorphism of Hercynian horneblende granodiorite beneath the blueschist facies Schistes Lustrés nappe of NE Corsica. J. Metam. Geol., 2: 95-113.

Gibbons W., Waters C. and Warburton J., 1986. The blueschist facies Schistes Lustrés of Alpine Corsica: a review. Geol. Soc. Am. Mem., 164: 301-331.

Gueguen E., Doglioni C. and Fernandez M., 1998. On the post-25 Ma geodynamic evolution of the western Mediterranean. Tectonophysics, 298: 259-269.

Gueydan F., Brun J-P, Phillippon M. and Noury M., 2017. Sequential extension as a record of Corsica rotation during Apennines slab roll-back. Tectonophysics, 710: 149-161..

Gueydan F., Leroy Y.M., Jolivet L. and Agard P., 2003. Analyses of continental midcrustal strain localization induced by microfaulting and reaction softening. J. Geophys. Res., 108: 2064-2081.

Guieu G., Loye-Pilot M.D., Lahondère D. and Ferrandini J., 1994. Carte géol. France (1/50000), feuille Bastia (1111). BRGM, Orléans, pp. 50

Handy M.R., Schmid S.M., Bousquet R., Kissling E. and Bernoulli D., 2010. Reconciling plate-tectonic reconstructions of Alpine Tethys with the geological-geophysical record of spreading and subduction in the Alps. Earth Sci. Rev., 102: 121-158.

Harris L., 1985. Progressive and polyphase deformation of the Schistes Lustrés in Cap Corse, Alpine Corsica. J. Struct. Geol., 7 (6): 637-650.

Jakni B., Poupeau G., Sosson M., Rossi P., Ferrandini J. and Guennoc P., 2000. Dénudations cénozoiques en Corse: une analyse thermochronologique par traces de fission sur apatites. C.R. Acad. Sci. Paris, 331: 775-782.

Jolivet J., 1993. Extension of thickened continental crust, from brittle to ductile deformation: examples from Alpine Corsica and Aegean Sea. Ann. Geofis., 36 (2): 139-153.

Jolivet L., Daniel J.M. and Fournier M., 1991. Geometry and kinematics of ductile extension in Alpine Corsica. Earth Planet. Sci. Lett., 104: 278-291.

Jolivet L., Dubois R., Fournier M., Goffé B., Michard A. and Jordan C., 1990. Ductile extension in Alpine Corsica. Geology, 18: 1007-1010.

Jolivet L., Faccenna C., Goffé B., Mattei M., Rossetti F., Brunet C., Storti F., Funiciello R., Cadet J.-P., D'Agostino N. and Parra T., 1998. Midcrustal shear zones in post-orogenic extension: Example from the Tyrrhenian Sea. J. Geoph. Res., 103: 12-123.

Jolivet L., Gorini C., Smit J. and Leroy S., 2015. Continental breakup and dynamics of rifting in back-arc basins: The Gulf of Lion margin. Tectonics, 34: 662-679.

Lacombe O. and Jolivet L., 2005. Structural and kinematic relationships between Corsica and the Pyreneeses-Provence domain at the time of the Pyrenean orogeny. Tectonics, 24: TC1003, doi: 10.1029/2004TC001673

Lagabrielle Y. and Lemoine M., 1997. Alpine, Corsican and Appennine ophiolites: the slowspreading ridge model. C.R. Acad. Sci. Paris, 325: 909-920.

Lagabrielle Y. and Polino R., 1988. Un schéma structural du domaine des Schistes Lustrés ophiolitifères au nord-ouest du massif du Mont Viso (Alpes sudoccidentales) et ses implications. C.R. Acad. Sci. Paris, 323: 957-964.

Lahondère D., and Guerrot C., 1997. Datation Sm-Nd du métamorphisme éclogitique en Corse alpine: un argument pour l'existence au Crétacé supérieur d'une zone de subduction active localisée sous le bloc corso-sarde. Géol. France, 3: 3-11.

Lahondère D., Rossi P. and Lahondère J.C., 1999. Structuration alpine d'une marge continentale externe: le massif du Tenda (Haute-Core). Implication géodynamiques au niveau de la transversale Corse-Appennins. Géol. France, 4: 27-44.

Lahondère J.C., Conchon O., Lahondère D., Dominici R. and Vautrelle C., 1983. Carte Géol. France (1/50000), feuille Bastia (1104). BRGM, Orléans.

Lanari P. and Duesterhoeft E., 2019. Modeling metamorphic rocks using equilibrium thermodynamics and internally consistent databases: Past achievements, problems and perspectives. J. Petrol., 60: 19-56.

Lanari P., Wagner T. and Vidal O., 2014. A thermodynamic model for di-trioctahedral chlorite from experimental and natural data in the system $MgO-FeO-Al_2O_3-SiO_2-H_2O$: applications to P-T sections and geothermometry. Contrib. Miner. Petrol., 167: 968.

Lapen T.J., Johnson C.M., Baumgartner L.P., Dal Piaz G.V., Skora S. and Beard B., 2007. Coupling of oceanic and continental crust during Eocene eclogite-facies metamorphism: evidence from Monte Rosa nappe, Western Alps. Contrib. Miner. Petrol., 153: 139-157.

Laporte D., Fernandez A. and Orsini J.B., 1991. Le complexe d'Ile Rousse, Balagne, Corse du Nord-Ouest: pétrologie et cadre de mise en place des granitoïdes magnésiopotassiques. Géol. France, 4: 15-30.

Lavier L. and Manatschal G., 2006. A mechanism to thin the continental lithosphere at magma-poor margins. Nature, 440 (7082): 324-328.

Law R.D., 2014. Deformation thermometry based on quartz c-axis fabrics and recrystallization microstructures: a review. J. Struct. Geol., 66: 129-161.

Levi N., Malasoma A., Marroni M., Pandolfi L. and Paperini M., 2007. Tectono- metamorphic history of the ophiolitic Lento Unit (northern Corsica): evidences for the complexity of accretion-exhumation processes in a fossil subduction system. Geod. Acta, 20 (1): 99-118.

Li X.H., Faure M., Rossi P., Lin W. and Lahondère D., 2015. Age of Alpine Corsica ophiolites revisited: Insights from in situ zircon U-Pb age and O-Hf isotopes. Lithos, 220: 179-190.

Maggi M., Rossetti F., Corfu F., Theye T., Andersen T.B. and Faccenna C., 2012. Clinopyroxene-rutile phyllonites from East Tenda Shear Zone (Alpine Corsica, France): pressure-temperature-time constraints to the Alpine reworking of Variscan Corsica. J. Geol. Soc., London, 169: 723-732.

Malasoma A. and Marroni M., 2007. HP-LT metamorphism in the Volparone Breccia (Northern Corsica, France): evidence for involvement of the Europe/Corsica continental margin in the Alpine subduction zone. J. Metam. Geol., 25: 529-545.

Malasoma A., Marroni M., Musumeci G. and Pandolfi L., 2006. High pressure mineral assemblage in granitic rocks from continental units, Alpine Corsica, France. Geol. J., 41: 49-59.

Malasoma A., Morelli G., Di Rosa M., Marroni M., Pandeli E., Principi G. and Pandolfi L., 2020. The stratigraphic and structural setting of metamorphic continental units from Alpine Corsica: clues from the area between Asco and Golo valleys (Central Corsica, France). J. Maps, 16 (2): 313-323.

Malavieille J., Chemenda A. and Larroque C., 1998. Evolutionary model for the Alpine Corsica: mechanism for ophiolite emplacement and exhumation of high-pressure rocks. Terra Nova, 10: 317-322.

Malusà M.G., Faccenna C., Baldwin S.L., Fitzgerald P.G., Rossetti,F., Balestrieri M.L., Danisik. M., Ellero A., Ottria G. and Piromallo C., 2015. Contrasting styles of (U)HP rock exhumation along the Cenozoic Adria-Europe plate boundary (Western Alps, Calabria, Corsica). Geochem. Geophys. Geosyst., 16: 1786-1824.

Malusà M., Polino R. and Zattin M., 2009. Strain partitioning in the axial NW Alps since the Oligocene. Tectonics, 28 (3), https://doi.org/10.1029/2008TC002370

Maluski H., 1977. Application de la méthode $^{40}Ar/^{39}Ar$ aux minéraux des roches cristallines perturbées par des événements thermiques et tectoniques en Corse. Ph.D. thesis, Univ. Montpellier.

Maluski H., Mattauer M. and Matte P.H., 1973. Sur la presence de decrochement alpins en Corse. C.R. Acad. Sci. Paris , 276: 709-712.

Manatschal G., 1995. Jurassic rifting and formation of a passive continental margin (Platta and Err nappes, Eastern Switzerland): geometry, kinematics and geochemistry of fault rocks and comparison with Galicia margin. Diss. ETH, Nr. 11188, Zurich.

Marino M., Monechi S. and Principi G., 1995. New calcareous nanofossil data on the Cretaceous-Eocene age of Corsican turbidites. Riv. Ital. Pal.. Strat., 101: 49-62.

Marroni M. and Pandolfi L., 2001. Debris flow and slide deposits at the top of the Internal Liguride ophiolitic sequence, Northern Apennines, Italy: a record of frontal tectonic erosion in a fossil accretionary wedge. Isl. Arc, 10: 9-21.

Marroni M. and Pandolfi L., 2003. Deformation history of the ophiolite sequence from the Balagne Nappe, northern Corsica: insights in the tectonic evolution of the Alpine Corsica. Geol. J., 38: 67-83.

Marroni M. and Pandolfi L., 2007. The architecture of an incipient oceanic basin: a tentative reconstruction of the Jurassic Liguria-Piemonte basin along the Northern Apennine-Alpine Corsica transect. Int. J. Earth Sci., 96: 1059-1078.

Marroni M., Meneghini F. and Pandolfi L., 2010. Anatomy of the Ligure-Piemontese subduction system: evidence from Late Cretaceous-Middle Eocene convergent margin deposits from Northern Apennines (Italy). Int. Geol. Rev., 10-12: 1160-1192.

Marroni M., Meneghini F. and Pandolfi L., 2017. A revised subduction inception model to explain the Late Cretaceous, double-vergent orogen in the pre-collisional Western Tethys: evidence from the Northern Apennines. Tectonics, 36: 2227-2249.

Marroni M., Moratti G., Costantini A., Conticelli S., Benvenuti M.G., Pandolfi L., Bonini M., Cornamusini G. and Laurenzi M.A., 2015. Geology of the Monte Amiata region, Southern Tuscany, Central Italy. Ital. J. Geosci., 134 (2): 171-199.

Marroni M., Pandolfi L. and Meneghini F., 2004. From accretion to exhumation in a fossil accretionary wedge: a case history from Gottero Unit (Northern Apennines, Italy). Geod. Acta, 17: 41-53.

Marroni M., Pandolfi L., and Perilli N., 2000. Calcareous nannofossil dating of the San Martino Formation from the Balagne ophiolite sequence (Alpine Corsica): comparison with the Palombini Shale of the Northern Apennine. Ofioliti, 25: 147-156.

Martin A.J., Rubatto D., Vitale Brovarone A. and Hermann J., 2011. Late Eocene lawsonite-eclogite facies metasomatism of a granulite sliver associated to ophiolites in Alpine Corsica. Lithos, 125: 620-640.

Masini E., Manatschal G. and Mohn G., 2013. The Alpine Tethys rifted margins: Reconciling old and new ideas to understand the stratigraphic architecture of magma-poor rifted margins. Sedimentology, 60 (1): 174-196.

Massonne H.J. and Schreyer W., 1987. Phengite geobarometry based on the limiting assemblage with k-feldspar, phlogopite, and quartz. Contrib. Miner. Petrol., 96: 212-224.

Mattauer, M. and Proust F., 1975. Données nouvelles sur l'evolution structurale de la Corse alpine, C. R. Acad. Sci. Paris, 281: 1681-1684.

Mattauer M. and Proust F., 1976. La Corse alpine: un modèle de genèse du métamorphisme haute pression par subduction de croute continentale sous du matérial océanique. C.R. Acad. Sci. Paris, 282: 1249-1252.

Mattauer M., Faure M. and Malavieille J., 1981. Transverse lineation and large-scale structures related to Alpine obduction in Corsica. J. Struct. Geol., 3: 401-409.

Mattauer M., Proust F. and Etchecopar A., 1977. Linéation "a" et mécanisme de cisellement simple liés au chevauchement de la nappe de Schistes Lustrés en Corse. Bull. Soc. Géol. France, 14: 841-945.

Meneghini F., Pandolfi L. and Marroni M., 2020. Recycling of heterogeneous material in the subduction factory: evidence from the sedimentary mélange of the Internal Ligurian Units, Italy. J. Geol. Soc., 177: 587-599.

Ménot R.P. and Orsini J.B., 1990. Evolution du socle anté-Stéphanien de Corse: événements magmatiques et métamorphiques. Schweiz. Miner. Petr., 70: 35-53.

Meresse F., Lagabrielle Y., Malavieille J. and Ildefonse B., 2012. A fossil ocean-continent transition of the Mesozoic Tethys preserved in the Schistes Lustrés nappe of northern Corsica. Tectonophysics, 579: 4-16.

Michard A., Chalouan A., Feinberg H., Goffé B. and Montigny R., 2002. How does the Alpine belt end between Spain and Morocco?. Bull. Soc. Géol. France, 173(1): 3-15.

Michard A. and Martinotti G., 2002. The Eocene unconformity of the Brianconnais domain in the French-Italian Alps, revisited (Marguareis massif, Cuneo); a hint for a Late Cretaceous-middle Eocene frontal bulge setting. Geodin. Acta, 15: 289-301.

Mohn G., Manatschal G., Beltrando M., Masini E. and Kusznir N., 2012. Necking of continental crust in magma-poor rifted margins: Evidence from the fossil Alpine Tethys margins. Tectonics, 31 (1): doi:10.1029/2011TC002961.

Mohn G., Manatschal G., Muntener O., Beltrando M. and Masini E., 2009. Unravelling the interaction between tectonic and sedimentary process during lithospheric thinning in the Alpine Tethys margins. Int. J. Earth Sci., 99: S75-S101.

Molli G., 2008. Northern Apennine-Corsica orogenic system: an updated overview. In: S. Siegesmund, B. Fugenschuh and N. Froitzheim (Eds.), Tectonic aspects of the Alpine-Dinaride-Carpathian System. Geol. Soc. London Spec. Publ., 298: 413-442.

Molli G. and Malavieille J., 2011. Orogenic processes and the Corsica/Apennines geodynamic evolution: insights from Taiwan. Int. J. Earth Sci., 100: 1207-1224.

Molli G. and Tribuzio R., 2004. Shear zones and metamorphic signature of subducted continental crust as tracers of the evolution of the Corsica/Northern Apennine orogenic system. In: G.I. Alsop, R.E. Holdsworth, K.J.W. McCaffrey and M. Handy, (Eds.), Flow processes in faults and shear zones. Geol. Soc. London Spec. Publ., 224: 321-335.

Molli G., Menegon L. and Malasoma A., 2017. Switching deformation mode and mechanisms during subduction of continental crust: a case study from Alpine Corsica. Solid Earth, 8: 767-788.

Molli G., Tribuzio R. and Marquer D., 2006. Deformation and metamorphism at the eastern border of Tenda Massif (NE Corsica): a record of subduction and exhumation of continental crust. J. Struct. Geol., 28: 1748-1766.

Nardi R., Puccinelli A. and Verani M., 1978. Carta geologica della Balagne "sedimentaria" (Corsica) alla scala 1:25.000 e Note Illustrative. Boll. Soc. Geol. It., 97: 3-22.

Ohnenstetter M., Ohnenstetter D., Rocci G., 1976. Étude des métamorphismes successifs des cumulats ophiolitiques de Corse. Bull. Soc. Géol. France, 18 (1): 115-134.

Padoa E., 1999. Les ophiolites du massif de l'Inzecca (Corse alpine): lithostratigraphie, structure géologique et évolution géodynamique. Géol. France, 3: 37-48.

Padoa E., Saccani E. and Durand-Delga M., 2001. Structural and geochemical data on the Rio Magno Unit: evidences for a new "Apenninic" ophiolitic unit in Alpine Corsica and its geodynamic implications. Terra Nova, 13: 135-142.

Padoa E., Saccani E. and Durand-Delga M., 2002. The Rio Magno Unit (Alpine Corsica): a review of its structural, stratigraphical and geochemical features and their geodynamic implications. Ofioliti, 27 (1): 31-42.

Pandeli E., Giusti R., Elter F.M., Orlando A. and Orti L. 2018. Structural setting and metamorphic evolution of a contact aureole: the example of the Mt. Capanne pluton (Elba Island, Tuscany, Italy). Ofioliti, 43 (1): 41-73.

Pandolfi L., Marroni M. and Malasoma A., 2016. Stratigraphic and structural features of the Bas-Ostriconi Unit (Corsica): paleogeographic implications. C.R. Geosci., 348: 630-640.

Paquette J.L., Ménot R.P., Pin C. and Orsini J.B., 2003. Episodic and short-lived granitic pulses in a post-collisional setting: evidence from precise U-Pb zircon dating through a crustal cross-section in Corsica. Chem. Geol., 198: 1-20.

Passchier C.W. and Trouw R.A.J., 2005. Microtectonics: Berlin, New York, Springer, 16, pp. 366.

Pequignot G.,1984. Métamorphisme et tectonique dans les Schistes Lustrés à l'Est de Corte (Corse). Ph.D. Thesis Univ. Claude-Bernard (Lyon), pp. 145

Péron-Pinvidic G. and Manatschal G., 2009. The final rifting evolution at deep magma-poor passive margins from Iberia-Newfoundland: A new point of view. Int. J. Earth Sci., 98: 1581-1597.

Plunder A., Agard P., Dubacq B., Chopin C. and Bellanger M., 2012. How continuous and precise is the record of P-T paths? Insights from combined thermobarometry and thermodynamic modelling into subduction dynamics (Schistes Lustrés, Western Alps). J. Metam. Geol., 30 (3): 323-346.

Plunder A., Agard P., Chopin C., Pourteau A. and Okay A.I., 2015. Accretion, underplating and exhumation along subduction interface: from subduction initiation to continental subuction (Tavsanli zone, W Turkey). Lithos, 226: 233-254.

Principi G. and Treves B., 1984. Il sistema corso-appenninico come prisma d'accrezione. Riflessi sul problema generale del limite Alpi-Appennini. Mem. Soc. Geol. It., 28: 49-576.

Principi G., Bortolotti V., Chiari M., Cortesogno L., Gaggero L., Marcucci M., Saccani E. and Treves B., 2004. The pre-orogenic volcano-sedimentary covers of the western Tethys oceanic basin: a review. Ofioliti, 29 (2): 177-211.

Ravna E.J.K., Andersen T.B., Jolivet L. and De Capitani C., 2010. Cold subduction and the formation of lawsonite-eclogite from prograde evolution of eclogitized pillow lava from Corsica. J. Metam. Geol., 28: 381-395.

Rehault J.P., Boillot G. and Mauffred A., 1984. The western Mediterranean Basin geological evolution. Mar. Geol., 55: 447-477.

Ribes C., Manatschal G., Ghienne J.-F., Karner G.D., Johnsonm C.A., Flgueredo P.H., Incerpi N. and Epin M.-E., 2019. The syn-rift stratigraphic recrord across a fossil hyper-extended rifted margin: the example of the northwestern Adriatic margin exposed in the Central Alps. Int. J. Earth Sci., 108 (6): 2071-2095.

Rosenbaum G., Lister G.S. and Duboz C., 2002. Relative motion of Africa, Iberia and Europe during Alpine orogeny. Tectonophysics, 359: 117-129.

Rossetti F., Glodny J., Theye T. and Maggi M., 2015. Pressure temperature deformation- time of the ductile Alpine shearing in Corsica from orogenic construction to collapse. Lithos, 218-219: 99-116.

Rossi P., Cocherie A. and Fanning M., 2015. Evidence in Variscan Corsica of a brief and voluminous Late Carboniferous to Early Permian volcanic-plutonic event contemporaneous with a high-temperature/low-pressure metamorphic peak in the lower crust. Bull. Soc. Géol. France, 186 (2-3): 171-192.

Rossi P., Durand-Delga M., Caron J.M., Guieu G., Conchon O., Libourel G. and Loye-Pilot M., 1994. Carte Géologique de la France (1/50,000), feuille Corte (1110). BRGM, Orléans.

Rossi P., Durand-Delga M., Lahondère J.C., Baud J.P., Eal E., Lahondère D., Laporte D., Lluch D., Loyle M.D., Ohnenstetter M. and Palagi P., 2001. Carte Géologique de la France (1/50,000), feuille Santo Pietro di Tenda (1106). BRGM, Orléans.

Rossi P., Oggiano G. and Cocherie A., 2009. A restored section of the "southern Variscan realm" the Corsica-Sardinia microcontinent. C.R. Geosci., 341: 224-238.

Saccani E., Padoa E. and Tassinari R., 2000. Preliminary data on the Pineto gabbroic massif and Nebbio basalts: progress toward the geochemical characterization of Alpine Corsica ophiolites. Ofioliti, 25: 75-86.

Saccani E., Principi G., Garfagnoli F. and Menna F., 2008. Corsica ophiolites: geochemistry and petrogenesis of basaltic and metabasaltic rocks. Ofioliti, 33 (2): 187-207.

Sagri M., Aiello E. and Certini L., 1982. Le unità torbiditiche cretacee della Corsica. Rend. Soc. Geol. It., 5: 87-91.

Sallarès V. and Ranero C.R., 2005. Structure and tectonics of the erosional convergent margin of Antofagasta, north Chile (23°30'S). J.Geophys. Res., 110: B06101.

Sanfilippo A. and Tribuzio R., 2013. Origin of olivine-rich troctolites from the oceanic lithosphere: a comparison between the Alpine Jurassic ophiolites and modern slow spreading ridge. Ofioliti, 38 (1): 89-99.

Sanfilippo A., Tribuzio R., Tiepolo M. and Berno D., 2015. Reactive flows as dominant evolution process in the lowernmost oceanic crust: evidence from olivine of the Pineto ophiolite (Corsica). Contrib. Miner. Petrol., 170 (4): 38

Schmid S. and Kissling E., 2000. The arc of the Western Alps in the light of geophysical data on deep crustal structure. Tectonics, 19: 62-85.

Schmid S.M., Pfiffner O.A., Froitzheim N., Schönborn G. and Kissling E., 1996. Geophysical-geological transect and tectonic evolution of the Swiss-Italian Alps. Tectonics, 15 (5): 1036-1064.

Speranza F., Villa I.M., Sagnotti L., Florindo F., Cosentino D., Cipollari P. and Mattei M., 2002. Age of the Corsica-Sardinia rotation and Liguro- Provençal Basin spreading: new paleomagnetic and Ar/Ar evidence. Tectonophysics, 347: 231-251.

Staub R., 1924. Der Bau der Alpen. Beitr. z. geol. Karte. Schweiz. neue Folge 52: 107.

Stipp M., Stünitz H., Heilbronner R. and Schmid S.M., 2002. Dynamic recrystallization of quartz: correlation between natural and experimental conditions. In: S. De Meer, M.R. Drury, J.H.P. De Bresser, G.M. Pennock (Eds.), Deformation mechanisms, rheology and tectonics: Current status and future perspectives. Geol. Soc. London Spec. Publ., 200:171-190.

Strzerzynski P., Guillot S., Leloup P.H., Arnaud N., Vidal O., Ledru P., Corrioux G. and Darmendrail X., 2012. Tectono-metamorphic evolution of Brianconnains zone (Modane-Aussois and Southern Vanoise units, Lyon Turin transect, Western Alps). J. Geodyn., 56-57: 55-75.

Treves B., 1984. Orogenic belts as accretionary prisms: the example of the Northern Apennines. Ofioliti, 9: 345-367.

Treves B. and Harper G.D., 1994. Exposure of serpentinites on the ocean floor: sequence of faulting and hydrofracturing in the Northern Apennine ophicalcites. Ofioliti, 19: 435-466.

Tribuzio R. and Giacomini F., 2002. Blueschist facies metamorphism of peralkaline rhyolites from Tenda crystalline massif (northern Corsica): evidence for involvement in the Alpine subduction event? J. Metam. Geol., 20: 513-526.

Trincal V. and Lanari P., 2016. Al-free di-trioctahedral substitution in chlorite and ferri-sudoite end-member. Clay Miner., 51: 675-689.

Vidal O. and Parra T., 2000. Exhumation paths of high-pressure metapelites obtained from local equilibria for chlorite-phengite assemblage. Geol. J., 35: 139-161.

Vidal O., De Andrade V., Lewin E., Munoz M., Parra T. and Pascarelli S., 2006. P-T-deformation-Fe^{3+}/Fe^{2+} mapping at the thin section scale and comparison with XANES mapping: application to a garnet-bearing metapelite from the Sambagawa metamorphic belt (Japan). J. Metam. Geol., 24: 669-683.

Vitale Brovarone A., Beltrando M., Malavieille J., Giuntoli F., Tondella E., Groppo C., Beyssac O. and Compagnoni R., 2011. Inherited Ocean-Continent Transition zones in deeply subducted terranes: Insights from Alpine Corsica. Lithos, 124: 273-290.

Vitale Brovarone A. and Herwartz D., 2013. Timing of HP metamorphism in the Schistes Lustrés of Alpine Corsica: new Lu-Hf garnet and lawsonite ages. Lithos, 172-173: 175-191.

Vitale Brovarone A., Beyssac O., Malavieille J., Molli G., Beltrando M. and Compagnoni R., 2012. Stacking and metamorphism of continuous segments of subducted lithosphere in a high-pressure wedge: The example of Alpine Corsica (France). Earth Sci. Rev., 116: 35-56.

Vitale Brovarone A., Picatto M., Beyssac O., Lagabrielle Y. and Castelli D., 2014. The blueschist-eclogite transition in the Alpine chain: P-T paths and the role of slow-spreading extensional structures in the evolution of HP-LT mountain belts. Tectonophysics, 615: 96-121.

von Huene R. and Scholl DW., 1991. Observations at convergent margins concerning sediment subduction, subduction erosion, and the growth of continental crust. Rev. Geophys., 29: 279-316.

Warburton J., 1986. The ophiolite-bearing Schistes Lustrés nappe in Alpine Corsica: a model for the implacement of ophiolites that have suffered HP-LT metamorphism. Geol. Soc. Am. Mem., 164: 313-331.

Waters C.N., 1990. The Cenozoic tectonic evolution of Alpine Corsica. J. Geol. Soc. London, 147: 811-824.

Whitney D. and Evans B., 2010. Abbreviations for names of rock-forming minerals. Am. Miner., 95: 185-187.

Zarki-Jakni, B. Van Der Beek P., Poupeau G., Sosson M., Labrin E., Rossi P. and Ferrandini J., 2004. Cenozoic denudation of Corsica in response to Ligurian and Tyrrhenian extension: results from apatite fission track thermochronology. Tectonics, 23: TC1003, doi: 10.1029/ 2003TC001535.